

1 The biostratigraphic record of Early Cretaceous to Paleogene relative sea-level
2 change in Jamaica

3 David P. Gold^{a,*} James P. G. Fenton^a, Manuel Casas-Gallego^a, Vibor Novak^a, Irene Pérez-Rodríguez^a,
4 Claudia Cetean^a, Richard Price^a, Nicole Nembhard^b, Herona Thompson^b

5

6

7 ^{a,*} CGG Robertson, Llandudno, North Wales LL30 1SA, United Kingdom

8

9 ^b Petroleum Corporation of Jamaica Ltd, 5th Floor PCJ Building, 36 Trafalgar Road, Kingston 10,

10 Jamaica

11

12

13

14 This article has been submitted for publication and will appear in a revised form in the Journal of
15 South American Earth Sciences. Please carefully note that subsequent versions of this manuscript may
16 have different content

* Corresponding author at: Robertson CGG, part of CGG GeoConsulting, Llandudno, North Wales LL30 1SA,
United Kingdom. Tel: +44 1492 581111

E-Mail address: David.Gold@CGG.com (David Gold)

17 **ABSTRACT**

18 The island of Jamaica forms the northern extent of the Nicaragua Rise, an elongate linear tectonic
19 feature stretching as far as Honduras and Nicaragua to the south. Uplift and subaerial exposure of
20 Jamaica during the Neogene has made the island rare within the Caribbean region, as it is the only area
21 where rocks of the Nicaragua Rise are exposed on land. Biostratigraphic dating and
22 palaeoenvironmental interpretations using larger benthic foraminifera, supplemented by planktonic
23 foraminifera, nannopalaeontology and palynology of outcrop, well and corehole samples has enabled
24 the creation of a regional relative sea-level curve with the identification of several depositional
25 sequences. This study recognises ten unconformity-bounded transgressive-regressive sequences which
26 record a complete cycle of relative sea level rise and fall. Sequences are recognised in the Early to
27 ‘middle’ Cretaceous (EKTR1), Coniacian-Santonian (STR1), Campanian (CTR1), Maastrichtian
28 (MTR1-2), Paleocene-Early Eocene (PETR1), Eocene (YTR1-3) and Late Eocene-Oligocene (WTR1).
29 These transgressive-regressive cycles represent second to fourth order sequences, although most tie to
30 globally recognised third order sequences. Comparisons of the Jamaican relative sea-level curve with
31 other published global mean sea-level curves show that local tectonics exerts a strong control on the
32 deposition of sedimentary sequences in Jamaica. The effects of these tectonic events are exaggerated
33 by contemporaneous global eustatic trends. The relatively low rates of relative sea-level rise calculated
34 from the regional relative sea-level curve indicate that carbonate production rates were able to keep
35 pace with the rate of relative sea-level rise accounting for the thick successions of Maastrichtian
36 carbonates and those of the Yellow and White Limestone Groups. Carbonate platform drowning
37 within the White Limestone Group during the Oligocene to Miocene is attributed to environmental
38 deterioration given the low rates of relative sea-level rise.

39

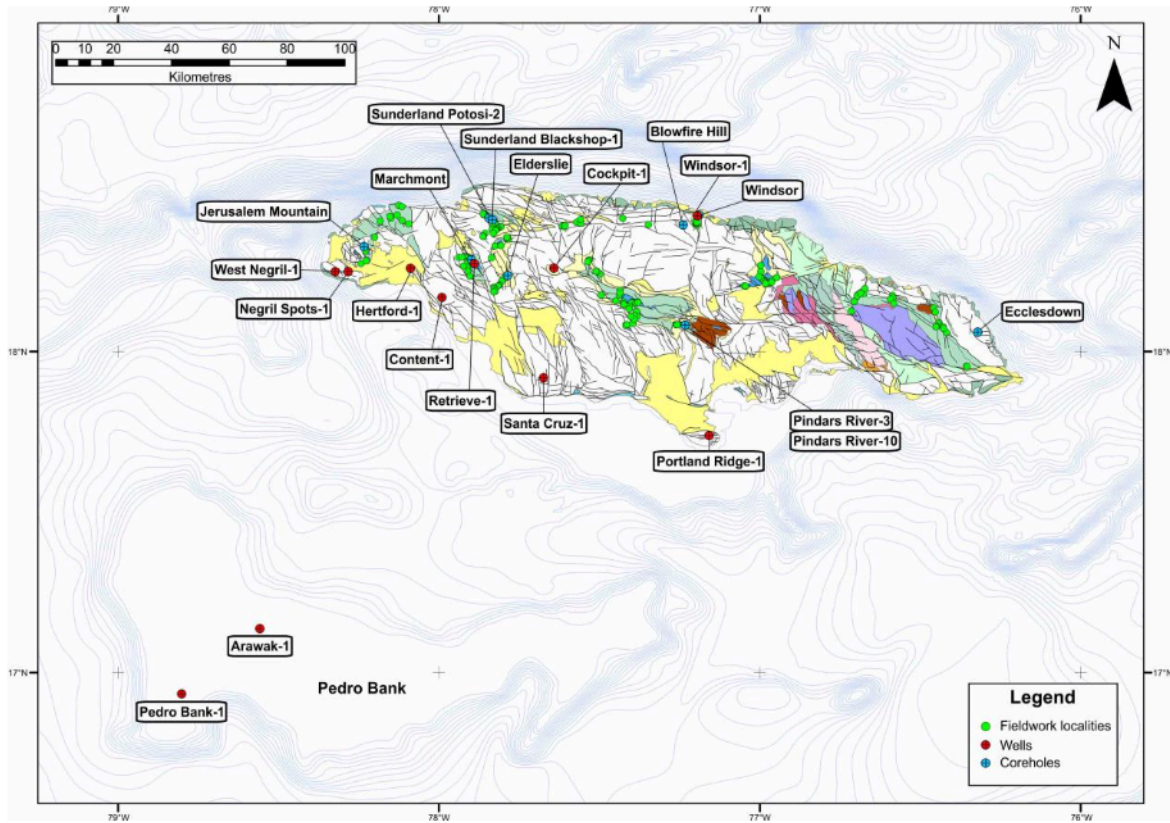
40 *Keywords:* Carbonates, biostratigraphy, foraminifera, relative sea-level, tectonics

41

42 **1. Introduction**

43 Jamaica is the third largest island in the Caribbean, behind Cuba and Hispaniola. It is situated in
44 the western portion of the Caribbean Sea and to the west of the Greater Antilles arc. The island of
45 Jamaica forms the northern extent of the Nicaragua Rise, an elongate linear feature stretching as far as
46 Honduras and Nicaragua to the southwest. The Nicaragua Rise is bounded on its northern side by the
47 Cayman Trough and is separated from the Cuban arc by the Yucatán Basin (Arden Jr., 1977). The
48 present day configuration of Nicaragua Rise comprises a shallow water carbonate platform up to
49 250 km in width, dropping steeply in to the Cayman Trough on its northern margin with a gentler
50 incline into the Colombian Basin on its southern side (Arden Jr., 1977). The island of Jamaica is rare
51 within the Caribbean region, as it is the only area where rocks of the Nicaragua Rise are exposed on
52 land.

53



54

55 **Fig. 1 – Geological map of Jamaica displaying locations of wells, coreholes and fieldwork**
56 **localities.**

57

58 Jamaica and its offshore sedimentary basins are sparsely explored, with only 2 wells drilled in
59 the offshore section and 9 wells onshore along with several shallow coreholes (Fig. 1). No wells have
60 been drilled since the mid-1980s. There have been oil or gas shows in 10 of the 11 wells drilled in the

61 onshore and offshore to date. The two wells drilled offshore Jamaica are Arawak-1 and Pedro Bank-1.
62 The following nine wells are onshore: Cockpit-1, Content A/Content-1, Hertford-1, Negril Spots-1
63 (formerly known as Jamaica-1), Portland Ridge-1, Retrieve-1, Santa Cruz-1, West Negril-1 and
64 Windsor-1. The distribution of all 11 wells across on- and offshore Jamaica is depicted in Figure 1.

65 The objective of this study is to describe new data from Jamaica which comprises new analyses
66 of over 800 outcrop and well/corehole samples. In addition, these new biostratigraphic and
67 sedimentological analyses revise and update the sequence-stratigraphic framework of Jamaica and tie
68 depositional cycles to third-order sequences of Hardenbol *et al.* (1998) recalibrated to the 2012
69 Geologic time scale (Gradstein *et al.*, 2012).

70

71 **2. Geological history**

72 Formation of Caribbean oceanic plateau or large igneous province (CLIP) which forms the
73 interior of the Caribbean Plate occurred during the early Jurassic (Burke *et al.*, 1978; Burke, 1988).
74 During the Early Cretaceous the crustal fragments that later assembled to form Jamaica and the
75 Nicaragua Rise were in a period of relative tectonic quiescence depositing the shallow marine
76 limestones of the Benbow Inlier, and similar rocks known from Puerto Rico and Trinidad, in vast
77 epeiric seas close to a volcanic arc (Kauffman and Sohl, 1974). Strata of the Benbow Inlier are the
78 oldest exposed in Jamaica, where there are no sediments older than Valanginian age (Brown and
79 Mitchell, 2010). Early to 'middle' Cretaceous volcanics in the Central Inlier and the succession of the
80 Benbow Inlier are interpreted to represent a volcanic island arc and/or ophiolite suite either as part of
81 the CLIP, or a back/fore-arc spreading centre (Wadge *et al.*, 1982; Jackson, 1987; Kerr *et al.*, 2004;
82 Mitchell, 2006). The Turonian-Coniacian unconformity is interpreted to have formed during the
83 assembly of CLIP fragments and subduction of normal ocean floor at convergent margins on the
84 northern and southern peripheries of the unusually buoyant CLIP ocean floor (Burke *et al.*, 1978;
85 Burke, 1988; Mitchell, 2006).

86 Following the formation of the Turonian-Coniacian unconformity deep water sedimentation was
87 prevalent over Jamaica during the Coniacian and Santonian. This deep water setting is responsible for
88 the deposition of the Windsor, Clamstead, Middlesex and Dias Formations. The transition to deep-
89 water siliciclastics of these units suggests rapid subsidence associated with continued intra-arc rifting.
90 A jump in the position of the magmatic arc during the latest Santonian, possibly related to the jarring
91 of buoyant CLIP arriving at the trench of the volcanic arc (Burke *et al.*, 1978), is responsible for the
92 formation of the early Campanian unconformity at the base of the Crofts Synthem (Mitchell, 2003).

93 Mitchell (2003; 2006) attributed the late Campanian to early Maastrichtian unconformity to the
94 collision between Caribbean Plate crustal fragments that make up the northern Nicaragua Rise and the
95 Maya/Yucatàn Block of the North American Plate. This event thrust island arc material over

96 underlying rocks of the CLIP. The late Campanian to early Maastrichtian unconformity is associated
97 with E-W trending thrust faults that form southward-verging imbricate thrust sheets onshore Jamaica
98 which potentially extend as far south as the lower Nicaragua Rise (Mitchell, 2003). The remnant thrust
99 sheets are now expressed as a series of E-W trending faults, which are the oldest structural features
100 found on Jamaica. This event is recognised by tectonic models of Burke (1988), Pindell and Barrett
101 (1990), Pindell (1994), Pindell and Kennan (2001; 2009), Kerr *et al.* (2004), Pindell *et al.* (2005) and
102 Mitchell (2006).

103 The late Maastrichtian ‘Kellits Synthem’ of Mitchell (2003) is reported to represent a single
104 major transgressive-regressive cycle (Mitchell and Blissett, 2001; Mitchell, 2003; 2006). This study
105 recognises two T-R cycles within the Maastrichtian. In the east of Jamaica, a suture is recorded in the
106 John Crow Mountain area between the characteristic island arc material that comprises the basement
107 of the majority of Jamaica with crust similar to that of Haiti (Lewis *et al.*, 2011). The suturing to the
108 east of Jamaica is attributed to south-westward subduction of CLIP crust beneath northeast Jamaica
109 initiating during the Maastrichtian (Arden Jr, 1977) and culminating in the formation of the
110 Cretaceous-Tertiary unconformity. Continued subduction and melting of the CLIP beneath northeast
111 Jamaica during the early Paleogene is responsible for the formation of the proto-Blue Mountains and
112 extrusion of exotic volcanics, such as adakites, within the Halberstadt Volcanics during the Early
113 Eocene (Hastie *et al.*, 2010a, 2010b, 2011) which may be responsible for the formation of an
114 unconformity recorded in eastern Jamaica at this time.

115 The unconformity between the Kellits Synthem and Middle Eocene strata of the Yellow
116 Limestone Group over much of western Jamaica (Clarendon and Hanover Blocks) is interpreted to
117 have formed during late Paleocene to Early Eocene northeast-southwest directed extension (Mitchell,
118 2003). This extension is related to sinistral strike-slip movement between the North American Plate
119 and the northern margin of the Caribbean Plate (Pindell, 1994; Mitchell, 2003). Extension occurred
120 over much of the Nicaragua Rise resulting in the formation of northwest-southeast trending horst and
121 graben structures such as the onshore Montpelier-Newmarket and Wagwater Troughs, and the offshore
122 Walton Basin and Pedro Bank horst. These grabens were filled with sediments shed from adjacent
123 highs, most notably Paleocene strata of the Wagwater Trough in the east of the island (Arden Jr.,
124 1969). Reactivation of NW-SE striking extensional faults to reverse faults during the Late Eocene
125 resulted in the denudation of the tops of sedimentary sections and may be responsible for the
126 unconformity between the White and Yellow Limestone units.

127 During the Neogene sinistral strike-slip motion along the boundary between the Jamaica plate
128 and Cayman Trough was transferred to the southern boundary of the Gonave Plate by fault
129 displacement through the Wagwater Trough (Mann *et al.*, 1985; 1995; DeMets and Wiggins-
130 Grandison, 2007; Abbott Jr. *et al.*, 2013). The collision and locking of the South Hispaniola, Gonave,
131 and lower Nicaragua Rise plates is believed to have caused this switch (DeMets and Wiggins-

132 Grandison, 2007). As a result, sinistral displacement passes through a restraining bend in the area of
133 the Blue Mountains, resulting in major transpression and causing significant uplift. The interaction of
134 Caribbean plates with Hispaniola also causes the regional uplift of Jamaica, with Campanian E-W
135 thrusts reactivated as strike-slip faults to further accommodate sinistral displacement.

136 The youngest tectonic event began in the Late Miocene, approximately 8-9 Ma, and is
137 continuing to the present day (Wright, 1971; Steineck, 1974; 1981; Katz and Miller, 1993).
138 Convergence of the North American Plate along the NW-SE oriented northern margins of Cuba and
139 Hispaniola resulted in a stress regime which is expressed by the Neogene uplift of Jamaica. This final
140 stage of tectonic deformation causes Plio-Pleistocene age carbonate terraces to be uplifted at a rate of
141 1.5mkyr^{-1} (Steineck, 1974; Katz and Miller, 1993; Cochran *et al.*, 2017) and regional NW directed
142 extension forming a large-scale structural trend that is broadly NE-SW. Within this stress regime the
143 E-W oriented former thrust sheets are reactivated as sinistral strike-slip faults and spectacular NE
144 verging folds within the Oligo-Miocene age Montpelier Formation are observed across the island.

145

146 **3. Material and methods**

147 This research forms part of a wider study evaluating the petroleum potential of Jamaica. During
148 this study, fieldwork was conducted in 2016 on the island of Jamaica (Fig. 1). During the fieldwork 60
149 formations were described and/or sampled, with over 200 samples collected from over 200 localities.
150 An additional 600 samples were collected from 10 Jamaican wells (Arawak-1, Cockpit-1, Content
151 A/Content-1, Hertford-1, Negril Spots-1 (formerly known as Jamaica-1), Portland Ridge-1, Retrieve-1,
152 Santa Cruz-1, West Negril-1 and Windsor-1) and 11 shallow coreholes (Blowfire Hill, Ecclesdown,
153 Elderslie, Jerusalem Mountain, Marchmont, Pindars River-3, Pindars River-10, Sunderland
154 Blackshop-1, Sunderland Potosi-2 and Windsor) provided by the Petroleum Corporation of Jamaica. In
155 addition, data from 11 DSDP and ODP wells (DSDP 151, 152, 153, 154/A, ODP 999A/B, 1000A/B,
156 1001A/B) were reviewed.

157 Samples were analysed for biostratigraphic dating using planktonic and larger benthic
158 foraminifera, palynomorphs and nannofossils. Ages have been established, wherever possible, from
159 the published ranges of regionally or globally recognised marker fossils. Important global references
160 for planktonic foraminifera include Sliter (1989) and Premoli Silva and Verga (2004) for the
161 Cretaceous, Olsson *et al.* (1999) for the Paleocene, and Pearson *et al.* (2006) for the Eocene. The
162 ranges of larger benthic foraminifera are taken from BouDagher-Fadel (2008), local references
163 (Hanzawa, 1962; Jiang and Robinson, 1987; Robinson and Wright, 1993; Krijnen *et al.*, 1993;
164 Robinson, 2004) and new interpretations of this study (Fig. 2). The planktonic foraminiferal zones
165 used in the Paleogene are those of Berggren *et al.* (1995) and Berggren and Pearson (2005),
166 recalibrated as sub-tropical foraminiferal Zones for the Cenozoic by Wade *et al.* (2011). Within the

183 Beavington-Penney and Racey (2004), Robinson (2004), Hohenegger (2005), Murray (2006),
184 BouDagher-Fadel (2008), Baker *et al.* (2009) and Mitchell (2013).

185 The island of Jamaica and the region of the northern Nicaragua Rise are described to have been
186 part of a continuous carbonate ‘megabank’ during the Paleogene (Droxler, 1991; 1993; Sigurdsson *et*
187 *al.*, 1997; Mutti *et al.*, 2005) therefore depositional settings are described using carbonate ramp
188 terminology, defined by Burchette and Wright (1992). Seven depositional settings were defined for the
189 purposes of this study including: terrestrial, paralic, proximal inner ramp, distal inner ramp, middle
190 ramp, outer ramp and basinal. Each depositional setting was assigned a water depth, and each sample
191 analysed was assigned to a depositional setting. Through biostratigraphic analyses the samples were
192 also assigned an age in Ma, based on the biozones they were allocated. Average water depths per Ma
193 were plotted as a graph to create a relative sea-level (RSL) curve. Standard error bars for each data
194 point on the sea-level curve incorporate the full range of environments interpreted for that period of
195 time by calculating the maximum, minimum and average bathymetry of all biostratigraphic control
196 points. In total 266 samples were assigned a depositional setting, bathymetry and biostratigraphic age
197 and were used to create the sea-level curve. This regional RSL curve was then compared to global sea-
198 level curves to assess potential timing of tectonic events.

199

200 **4. Depositional sequences**

201 Environmental preferences of organisms identified during biostratigraphic analyses permit the
202 construction of a RSL curve for the island of Jamaica (Figs. 3-6). The highest resolution of data points
203 occur during the Maastrichtian, Middle to Late Eocene and Oligocene. The RSL curve reveals ten
204 unconformity-bounded transgressive-regressive (T-R) depositional cycles which record a complete
205 cycle of relative sea level rise and fall in the stratigraphy of Jamaica. Commonly, only the
206 transgressive deposits are preserved, as strata deposited in the regressive phase of the previous
207 sequence are eroded during transgressive reworking and production of transgressive ravinement
208 surfaces. Maximum transgressive and regressive inflections in the RSL curve are associated with third-
209 order sequences. However, the deposition of each sequence may be controlled by interplay between
210 regional tectonic activity and global eustatic trends.

211 Single T-R cycles are identified within the Early Cretaceous (EKTR1), Santonian (STR1) and
212 Campanian (CTR1), two T-R cycles are identified in the Maastrichtian (MTR1, MTR2), a further
213 single T-R cycle within the Paleocene-Early Eocene (PETR1), three T-R cycles within the
214 Middle Eocene age Yellow Limestone Group (YTR1, YTR2, YTR3) and a single transgressive
215 sequence within the Late Eocene to Miocene age White Limestone Group (WTR1). Transgressions
216 and regressions that are recorded within the Yellow Limestone Group represent changes in RSL of
217 only several tens of metres. The White Limestone Group sequence WTR1 indicates a longer term,

218 lower-order, transgressive sequence than the shorter time-span Yellow Limestone Group sequences.
219 This implies a longer term tectonic control on the deposition of these units, interpreted to be associated
220 with the opening of the Cayman Trough.

221

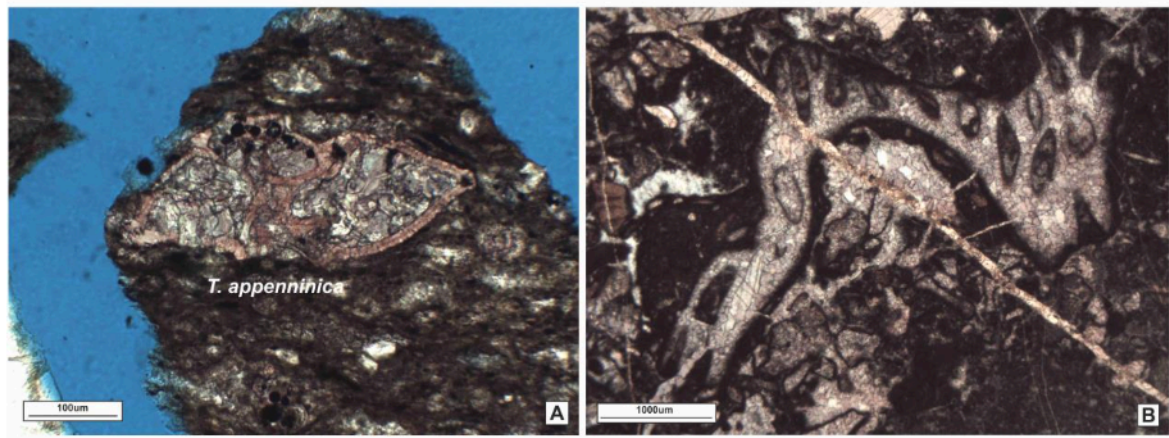
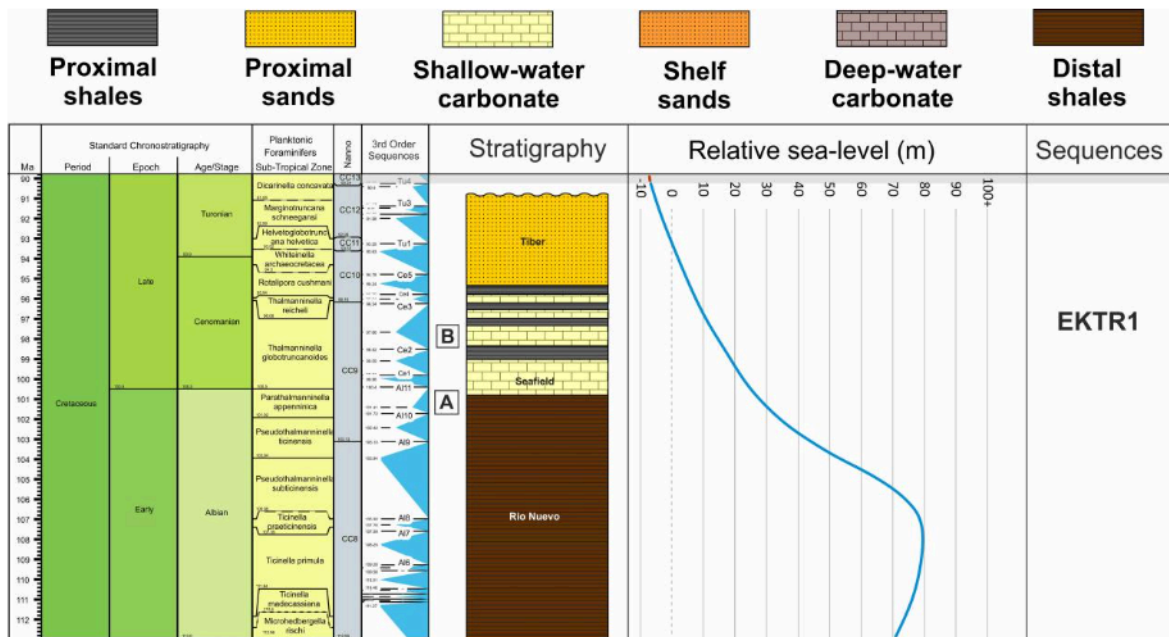
222 4.1. Early Cretaceous (EKTR1)

223 The Early Cretaceous T-R cycle (EKTR1) is identified through biostratigraphic and
224 sedimentological analyses to reach average water depths of approximately 80m at the maximum
225 transgressive inflection of the RSL curve, interpreted to coincide with the Al8 (103.94 Ma) maximum
226 flooding surface (MFS) of Hardenbol *et al.* (1998). The regressive phase of the RSL curve from the
227 late Albian to late Turonian attains average water depths of less than 10m coinciding with the Tu4
228 (90.25 Ma) sequence boundary (SB) of Hardenbol *et al.* (1998). The EKTR1 sequence is represented
229 by the Rio Nuevo Formation and Seafield Limestone. The EKTR sequence is observed within the
230 Retrieve-1 and Windsor-1 wells.

231 The Rio Nuevo Formation contains a basal shale unit containing carinate planktonic
232 foraminifera, including *Thalmaninella appenninca* spp. (Fig. 3), and globular morphologies. In
233 addition, radiolaria and calcareous nannofossils are also abundant. This fossil assemblage and fine-
234 grained laminated nature of the groundmass suggests deposition within a distal, low energy setting
235 such as an outer ramp or basinal environment. A certain degree of terrigenous input is interpreted
236 based on the occurrence of land-derived and water-transported fern spores in the palynological
237 assemblages, such as *Deltoidospora* spp. and *Echinatisporis* spp.

238 Interbedded shallow water carbonates and organic-rich mudstones of the Seafield Limestone are
239 observed in outcrop towards the top of the Rio Nuevo Formation suggesting periodic shallowing
240 sequences associated with minor oscillations within the RSL trend. Similar interbedded limestones and
241 organic-rich shales are observed in Albian to Cenomanian age strata in the Windsor-1 and Retrieve-1
242 wells and are interpreted to be coeval with Rio Nuevo and Seafield Limestone. Limestone interbeds
243 contain an assemblage of shallow water rudist bivalves (Fig. 3) and predominantly agglutinated
244 foraminifera indicating deposition within an oligotrophic, inner ramp setting. The interbedded
245 organic-rich black shales are interpreted to correlate to highly restricted, anoxic, estuarine or lagoonal
246 sediments. The occurrence of superabundant amorphous organic matter within the black shales
247 suggests oxygen-deficient bottom conditions.

248



249
 250 **Fig. 3 – Jamaican RSL curve of the Early to ‘middle’ Cretaceous (EKTR1 sequence). The**
 251 **highest sea-level is associated with the A18 MFS with the regressive phase culminating with the**
 252 **formation of the Tu4 SB. A) The planktonic foraminifera *Thalmanninella appenninica* are**
 253 **observed within the top of the Rio Nuevo Formation in the Retrieve-1 well, B) Caprinid rudists**
 254 **and dasycladacean green algae occur within the Seafield Limestone of the Windsor-1 well.**
 255

256 The overall shallowing upwards sequence of outer ramp shales, replaced by the inner ramp
 257 Seafield Limestone interbedded with marginal marine organic-rich shales throughout the entire Rio
 258 Nuevo Formation is correlated to the regressive phase of the EKTR1 sequence (Fig. 3). An
 259 unconformity separating Benbow Inlier strata from strata of the St. Ann’s Great River and Lucea
 260 Inliers (Grippi, 1978; Mitchell *et al.*, 2011) is identified from the Turonian and Coniacian. This
 261 unconformity lasts a duration of 2.39 Ma and occurs between the Tu4 to Co1 sequence boundaries
 262 (90.25 to 87.86 Ma) where part of the *Dicarinella concavata* micropalaeontological Zone is missing.

263

264 4.2. *Santonian (STR1)*

265 The Late Cretaceous, Santonian T-R cycle (STR1) initiates at the Co1 SB of Hardenbol *et al.*
266 (1998), reaching average water depths of approximately 80m at the maximum transgressive inflection
267 of the RSL curve correlated to the Co1 MFS (86.92 Ma). The regressive phase of the STR1 sequence
268 culminates with the Sa3 SB (84.08 Ma) where subaerial exposure of Jamaica resulted in the formation
269 of the early Campanian unconformity. The STR1 sequence is represented by the Windsor and
270 Clamstead Formations of the St. Ann's Great River Inlier and the Middlesex and Dias Formations of
271 the Lucea Inlier, Retrieve-1 and Windsor-1 wells, and Sunderland Blackshop-1 and Windsor
272 coreholes.

273 Interbedded sandstone/conglomerate and shale units within the Windsor Formation are
274 interpreted as fining and deepening upwards sequences. Thick sandstone and conglomerate beds at the
275 base of the Windsor sequence are interpreted to originate as shelf sands, with possible submarine
276 volcanic material transported as sediment gravity flows causing emplacement of mudstone rip-up
277 clasts (Mitchell *et al.*, 2011). The homogeneous nature of thick fine-grained sediments of the overlying
278 Clamstead Formation suggests continued deposition under persistent low energy conditions. The
279 abundance of carinate foraminifera including *Contusotruncana fornicata*, *C. morozovae*, *Dicarinella*
280 *asymetrica*, *D. concavata*, *Marginotruncana marginata*, *M. pseudolinneiana*, *M. renzi*, *M.*
281 *schneegansi*, *M. sigali*, *M. sinuosa*, *M. tarfayaensis*, *M. undulata*, *Whiteinella aumalensis* and
282 *Whiteinella baltica* observed within fine-grained units of the Windsor and Clamstead Formations
283 suggest deposition occurred in a distal marine, outer ramp to basinal setting associated with the Co1
284 MFS (Fig. 4).

285 Sedimentary structures such as groove and flute casts, and repetitive fining upwards Bouma
286 sequences, within the Dias and Middlesex Formations suggest these units were deposited as deep-
287 water turbidites. This interpretation supports that of Grippi (1978). The deposition of these deep-water
288 turbidites is interpreted to be coeval with sediment gravity flows within the Windsor Formation and is
289 also interpreted to correspond to the Co1 MFS within the STR1 sequence (Fig. 4). The early
290 Campanian unconformity (Sa3 to Cam2, ca. 84.08 to 81.53 Ma) which lasted a duration of at least 2.55
291 Ma where nannofossil zone CC17 is missing occurs between sediments of the STR1 and CTR1
292 sequence.

293

294 4.3. *Campanian (CTR1)*

295 The Campanian T-R cycle (CTR1) initiates at the Cam2 SB (81.53 Ma), reaching average water
296 depths of 35m at the maximum transgressive inflection of the RSL curve correlated to the Cam5 MFS
297 (79.28 Ma). The regressive phase of the CTR1 sequence culminates with the Cam9 SB (73.91 Ma),

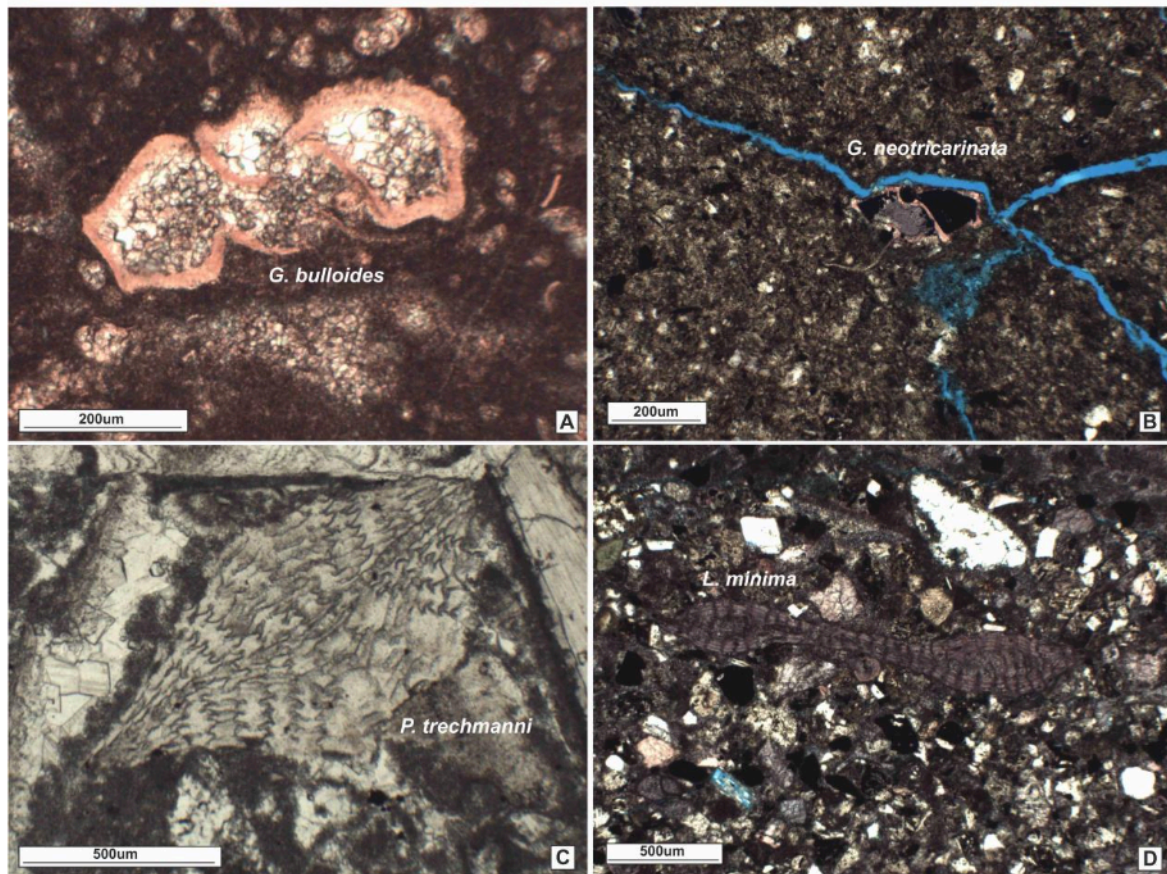
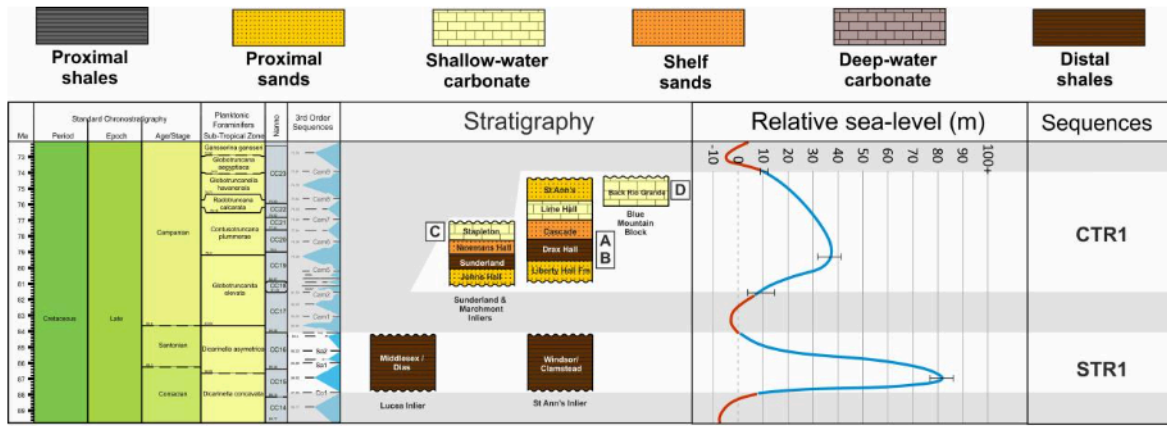
298 reaching average water depths of 15m before further subaerial exposure of Jamaica resulted in the
299 formation of the Maastrichtian-Campanian unconformity (Fig. 4). The CTR1 sequence is represented
300 by the Campanian age successions of the St. Ann's Great River, Sunderland and Marchmont Inliers,
301 Retrieve-1, West Negril-1 and Windsor-1 wells, and Marchmont, Sunderland Blackshop-1, Sunderland
302 Potosi-2 and Windsor coreholes

303 The T-R cycle of the CTR1 sequence is best displayed within the Sunderland and Marchmont
304 Inliers. Here, the base of the John's Hall Formation comprises a basal conglomerate that contains large
305 clasts and foraminiferal assemblage which suggests a proximal, marginal marine depositional
306 environment. The conglomerate contains occasional *Pseudorbitoides chubbi* which restricts the age of
307 this unit to the early Campanian (Jiang and Robinson, 1987; Krijnen *et al.*, 1993) and may represent a
308 basal conglomerate lag at the beginning of the CTR1 transgressive sequence which passes upwards to
309 deep-water shales within the Johns Hall Formation.

310 The deposition of the Sunderland Formation continues the deepening upwards trend from the
311 proximal Johns Hall Formation. The presence of *Planolites* ichnotaxa observed within the Sunderland
312 Formation suggests deposition within the mid to distal continental shelf (Benton and Harper, 1997).
313 Globular planktonic foraminifera including *Heterohelix* spp. and *Muricohedbergella* spp. and lack of
314 carinate morphologies within this unit also indicate moderate water depths of the middle to outer shelf
315 (e.g. Bé, 1977). This formation represents maximum transgressive point within the CTR1 sequence,
316 corresponding to the Cam5 MFS, and is interpreted to be contemporaneous with the Drax Hall
317 Formation of the St. Ann's Great River Inlier (Fig. 4). Planktonic foraminifera, such as *Globotruncana*
318 spp. (Fig. 4), and spherical radiolaria are common within the Drax Hall Formation. The presence of
319 *Globotruncana neotricarinata* in the Drax Hall Formation (Fig. 4) constrains the formation to a
320 Campanian age, ranging from the *Globotruncanita elevata* Zone to either the *Radotruncana calcarata*
321 or *Gansserina gansseri* Zones in stratigraphic sections from the Exmouth Plateau and Italy,
322 respectively (Petruzzo *et al.*, 2011).

323 In the Sunderland and Marchmont Inliers, the Sunderland Formation is overlain by the
324 Newman's Hall Formation. The Newman's Hall Formation is described as comprising transitional
325 shelfal sands deposited between the deep water shales of the underlying Sunderland Formation and
326 overlying shallow water Stapleton Limestone (Krijnen *et al.*, 1993). This formation is interpreted to
327 mark the start of the regressive phase of the CTR1 sequence. Based on the Newman Hall Formation's
328 stratigraphic position above the Sunderland Formation, it is interpreted to be middle Campanian age.

329 The Stapleton Formation overlies the Newmans Hall Formation to the south of the Sunderland
330 Inlier. This formation comprises fossiliferous limestone which contains a diverse assemblage of large
331 rudist bivalves including radiolitids, caprinids, plagiptychids and hippuritids, particularly specimens
332 of *Barrettia* spp., echinoids and larger benthic foraminifera. Limestones of the Stapleton Formation
333 contain occasional specimens of *Pseudorbitoides trechmanni* (Fig. 4). The presence of this taxon
334 restricts the age of the Stapleton Formation to the middle Campanian (Jiang and Robinson, 1987;
335 Krijnen *et al.*, 1993). The microfossil assemblage suggests deposition within a shallow marine setting.
336 The fragmented nature of the bioclasts indicates a moderate degree of hydrodynamic energy.
337 Therefore, it is interpreted that the Stapleton Formation was deposited in a distal inner ramp setting
338 approaching fair-weather wave base.



339
 340 **Fig. 4 – Jamaican RSL curve of the Coniacian to Campanian (STR1 and CTR1 sequences). High**
 341 **sea-level correlates with the Co1 MFS in the STR1 sequence and Cam5 MFS in the CTR1**
 342 **sequence. The planktonic foraminifera *Globotruncana bulloides* (A) and *Globotruncana***
 343 ***neotricarinata* (B) occur within the Drax Hall Formation. The larger benthic foraminifera**
 344 ***Pseudorbitoides trechmanni* (C) and *Lepidorbitoides minima* (D) within the Stapleton Limestone**
 345 **and Back Rio Grande Formation are characteristic of the middle to late Campanian.**
 346

347 The Stapleton Formation is interpreted to be a diachronous equivalent of the Lime Hall
 348 Formation of the St. Ann's Great River Inlier. The Lime Hall Formation contains a similar fossil

349 assemblage including rudist bivalves such as *Barrettia* spp. and common larger benthic foraminifera.
350 The presence of *Pseudorbitoides* spp. observed within the Lime Hall Formation indicates it is no
351 younger than late Campanian age (Mitchell and Ramsook, 2009). However, Mitchell *et al.* (2011) note
352 an absence of *Pseudorbitoides* within the Lime Hall Formation which is interpreted here to be due to
353 sampling, rather than stratigraphic, reasons as this taxon is observed in this study. Nevertheless, a late
354 Campanian age for the age of the Lime Hall Formation is consistent with Mitchell *et al.* (2011). The
355 Stapleton and Lime Hall Formations are interpreted to be diachronous equivalents of the Back Rio
356 Grande Formation of the Blue Mountain Block (Fig. 4). Samples within the Back Rio Grande
357 Formation contain *Orbitoides megaliformis* and *Lepidorbitoides minima* (Fig. 4), the latter reported as
358 an index fossil for the Campanian found associated with late Campanian planktonic foraminifera in
359 Europe (Aguilar *et al.*, 2002). Therefore, the Back Rio Grande Formation is interpreted to be late
360 Campanian age. This is consistent with the age of the formation assigned by Mitchell and Ramsook
361 (2009).

362 The Stapleton, Lime Hall and Back Rio Grande Formations represent a shallow water facies at
363 the top of the St. Ann's Great River, Sunderland and Marchmont Inliers' regressive phase of the CTR1
364 sequence. This sequence shallows upwards from the deep water Sunderland and Drax Hall
365 Formations, whose deposition is associated with the Cam5 MFS. The late Campanian to early
366 Maastrichtian unconformity is interpreted to occur between sequence boundaries Cam9 and Ma1
367 (73.91 to 72.05 Ma), lasting a duration of at least 1.86 Ma, where parts of the *Globotruncana*
368 *aegyptiaca* to *Gansserina gansseri* micropalaeontological zones are absent.

369

370 4.4. Maastrichtian 1 (MTR1)

371 The first Maastrichtian T-R cycle (MTR1) initiates at the Ma1 SB (72.05 Ma), reaching average
372 water depths of 85m at the maximum transgressive inflection of the RSL curve correlated to the Ma1
373 MFS (70.66 Ma). The regressive phase of the MTR1 sequence culminates with the Ma2 SB (69.27
374 Ma) reaching average water depths of 5m before the transgression of the second Maastrichtian T-R
375 cycle (Fig. 5). The MTR1 sequence is represented by the early to mid Maastrichtian age successions
376 of the Jerusalem Mountain, Sunderland, Marchmont, Carlton Hill and Maldon Inliers, Blue Mountain
377 Block, Cockpit-1, Content-1/A, Hertford-1, Negril Spots-1, Retrieve-1 and West Negril wells, and
378 Jerusalem Mountain corehole.

379 In the Sunderland and Marchmont Inliers the MTR1 sequence commences with the deposition
380 of the Shepherds Hall Formation. The Shepherds Hall Formation comprises a polymict, matrix-
381 supported conglomerate consisting of medium-grained sandstone supporting centimetre scale
382 subangular clasts. The Shepherds Hall Formation fines upwards towards a fine-grained, well sorted
383 sandstone with internal millimetre scale ripple cross laminations. Based on the presence of

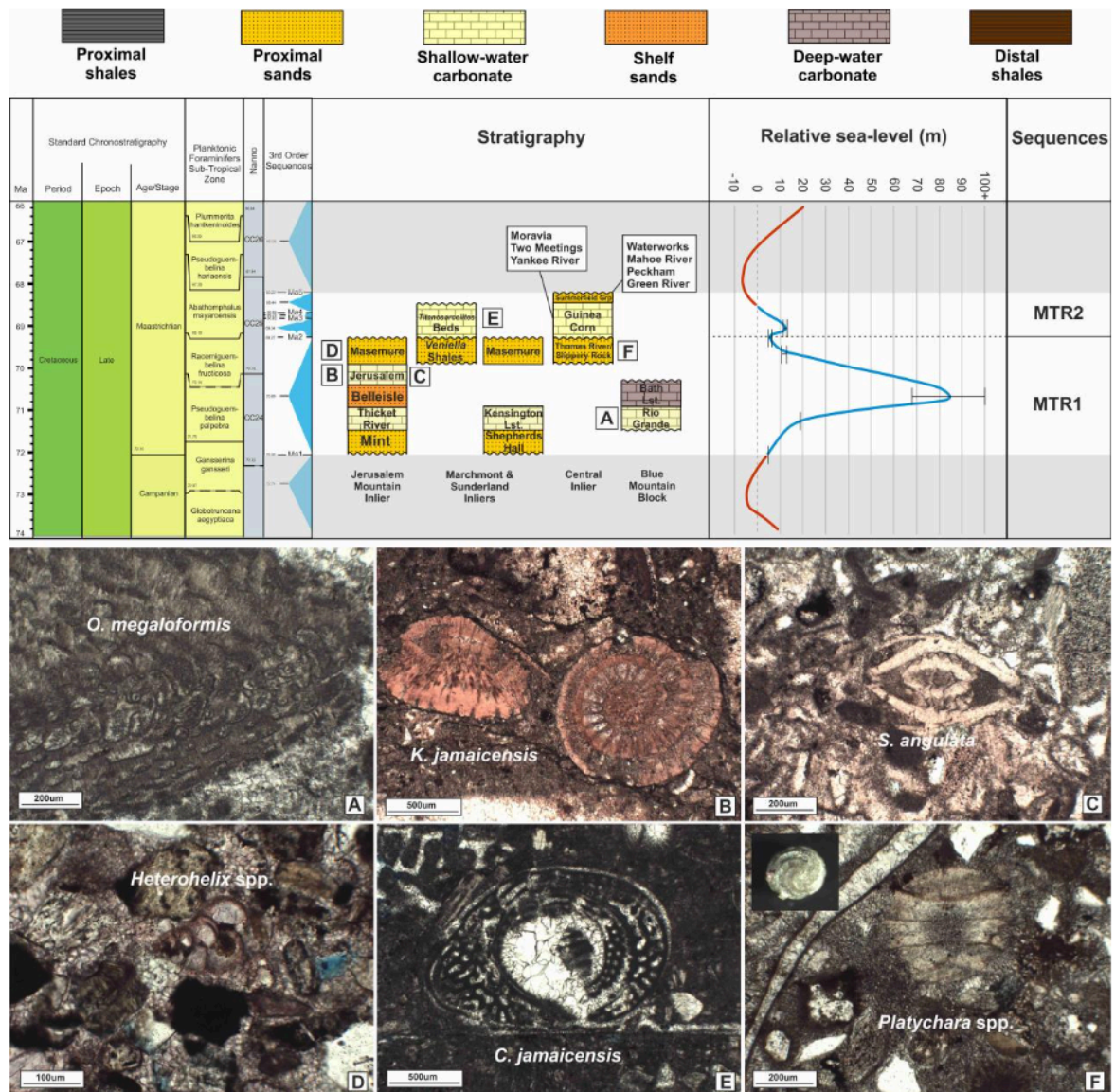
384 conglomerates and ripple laminations, this formation is interpreted to have been deposited in a fluvio-
385 deltaic setting where conglomerates represent a basal conglomerate lag at the base of the transgressive
386 phase of the MTR1 sequence. The Shepherds Hall Formation may also be a direct equivalent of the
387 marginal marine Mint Formation of the Jerusalem Mountain Inlier (Mitchell and Edwards, 2016).

388 Limestones of the Thicket River Formation and Kensington Limestone overlie the Mint and
389 Shepherds Hall Formations in the Jerusalem Mountain and Sunderland/Marchmont Inliers,
390 respectively. These limestones contain a diverse fossil assemblage including rudist bivalves,
391 particularly *Trechmannites rudissimus*, dasycladacean algae, miliolid foraminifera and gastropods
392 which indicate photic, oligotrophic conditions with normal marine salinities. The highly fragmented
393 nature of the bioclasts indicates high levels of hydrodynamic energy. Therefore, it is interpreted that
394 the Thicket River Formation and Kensington Limestone was deposited in a distal, inner ramp setting
395 approaching fair-weather wave base, marking a marginal deepening upwards trend from the
396 underlying Mint and Shepherds Hall Formations. In the Blue Mountain Block the limestones of the
397 Thicket River Formation and Kensington Limestone are coeval with the Rio Grande Formation which
398 contains a benthic foraminiferal assemblage that includes *Orbitoides megaliformis* (Fig. 5),
399 *Fissoelphidium operculiferum*, *Rotalia skourensis* and *Montcharmontia appenninica*, indicative of a
400 Maastrichtian age.

401 The transgressive phase of the MTR1 sequence culminates with the deposition of relatively
402 deeper water, middle to outer ramp, deposits of the Belleisle Formation in the Jerusalem Mountain
403 Inlier. The Belleisle Formation may be a lateral equivalent to planktonic foraminifera-rich Bath
404 Limestone of the Blue Mountain Block. The Bath Limestone contains abundant globotruncanid
405 planktonic foraminifera including *Abathomphalus intermedius*, *Contusotruncana contusa* and
406 *Globotruncana bulloides*. This assemblage is restricted to the *Abathomphalus mayaroensis* –
407 *Pseudoguembelina palpebra* micropalaeontological zones, confirming the absence of the *Gansserina*
408 *gansseri* zone at the Campanian-Maastrichtian unconformity and the upper zones of the Maastrichtian
409 absent at the Cretaceous-Tertiary unconformity. Both the Belleisle Formation and Bath Limestone
410 mark the maximum transgressive inflection of the MTR1 sequence, interpreted to correspond to the
411 Ma1 MFS (Fig. 5).

412 The Belleisle Formation is overlain by the Jerusalem Formation (Mitchell and Edwards, 2016),
413 which marks the start of the shallowing upwards, regressive phase of the MTR1 sequence. The
414 Jerusalem Formation contains rudist bivalves, gastropods, oysters, algal material and larger benthic
415 foraminifera commonly *Kathina jamaicensis* and *Sulcoperculina angulata* (Fig. 5) which are typical of
416 Maastrichtian age strata in Jamaica (e.g. Brown and Bronnimann, 1957). The regressive phase of the
417 MTR1 sequence is interpreted to follow the Ma1 MFS and terminate at the Ma2 sequence boundary
418 (Fig. 5).

419



420
 421 **Fig. 5 – Jamaican RSL curve of the Maastrichtian (MTR1-2 sequences). High sea-level of the**
 422 **MTR1 sequence correlates with the Ma1 MFS. Two transgressive-regressive cycles occur within**
 423 **the Maastrichtian. The larger benthic foraminifera *Orbitoides megaliformis* (A), *Kathina***
 424 ***jamaicensis* (B) and *Sulcoperculina angulata* (C) are common in Maastrichtian strata from**
 425 **Jamaica. Immature calcite cemented sandstones of the Masemure Formation contain rare**
 426 **planktonic foraminifera including *Heterohelix* spp. (D). The miliolid foraminifer *Chubbina***
 427 ***jamaicensis* (E) is an index fossil for the late Maastrichtian observed within the *Titanosarcollites***
 428 **beds. Freshwater charophytes including *Platychara* spp. (F) occur within the Slippery Rock**
 429 **Formation indicating terrestrially influenced deposition.**

430

431 4.5. *Maastrichtian 2 (MTR2)*

432 The second Maastrichtian T-R cycle (MTR2) initiates at the Ma2 SB (69.27 Ma), reaching
433 average water depths of 12m at the maximum transgressive inflection of the RSL curve correlated to
434 the Ma2 MFS (69.04 Ma). The regressive phase of the MTR2 sequence culminates with the Ma5 SB
435 (68.20 Ma) where terrestrially influenced strata top the sequence (Fig. 5). The MTR2 sequence is best
436 represented by mid to late Maastrichtian age successions of the Sunderland, Marchmont and Central
437 Inliers, Cockpit-1, Content-1/A, Hertford-1, Negril Spots-1, Retrieve-1 and West Negril wells.

438 The MTR2 sequence commences with deposition of the Masemure, Slippery Rock and Thomas
439 River Formations, and the *Veniella* Shales. The Masemure Formation comprises well-sorted, fine-
440 grained sandstone to siltstone. Grains are sub angular with moderate sphericity comprising quartz,
441 plagioclase feldspar and clay minerals including chlorite within calcite cement. Masemure Formation
442 sediments are therefore classified as texturally and mineralogically immature sandstones. Mitchell and
443 Edwards (2016) report that the Masemure Formation does not yield fossils, yet samples from this
444 formation analysed by this study recorded *Rotalia skourensis* and *Heterohelix* spp. (Fig. 5), indicative
445 of a Maastrichtian age. This unit shares lithological characteristics to the *Veniella* shales which contain
446 large bivalves including *Veniella/Roudairia* spp. The bivalves *Veniella/Roudairia* are reported from
447 shallow marine deposits in California (Kirby and Saul, 1995). The immaturity of the microfaunal
448 assemblage of the Masemure Formation suggests deposition within a marginal, paralic, marine
449 environment. The Masemure Formation is also correlated to the Thomas River Formation (Mitchell
450 and Edwards, 2016) and Slippery Rock Formation. Asymmetrical ripples on bedding surfaces
451 observed at the Slippery Rock Formation type section indicate deposition under a unidirectional
452 current presently directed to the north. It is interpreted that this is a fluvial deposit, which is further
453 supported by the presence of freshwater charophytes (Fig. 5), particularly *Platychara* spp. and *Azolla*
454 spp. spores (Peck and Forester, 1979; Kumar and Grambast-Fessard, 1984; Kumar and Oliver, 1984).
455 It is interpreted that the Masemure, Slippery Rock and Thomas River Formations, and the *Veniella*
456 Shales were deposited at the maximum regressive inflection of the Jamaican RSL curve between the
457 MTR1 and MTR2 sequences, associated with the Ma2 SB.

458 The Slippery Rock and Thomas River Formations, and the *Veniella* Shales, are overlain by
459 rudist limestones of the Guinea Corn Formation and *Titanosarcolites* Beds in the Sunderland,
460 Marchmont and Central Inliers. The *Titanosarcolites* Beds contain a fossil assemblage characterised
461 by rudist bivalves *Titanosarcolites*, *Thyrastylon*, *Trechmannites* and *Oligosarcolites*, which are often
462 preserved in life position, dasycladacean green algae and common miliolid foraminifera, including
463 *Kathina jamaicensis* and *Chubbina jamaicensis* (Fig. 5), indicating deposition in a shallow, photic and
464 oligotrophic marine setting. Mitchell (2005) suggests *Chubbina* is an index fossil for the late

465 Maastrichtian. It is interpreted that the *Titanosarcolites* Beds were deposited in a proximal inner ramp
466 setting.

467 The Guinea Corn Formation is also dominated by a rudist bivalve assemblage including
468 *Chiapasella radiolitiformis* and *Titanosarcolites* spp. Larger benthic foraminifera including *Orbitoides*
469 *megaliformis* and *Lepidorbitoides* spp. are also observed. The foraminifer *Orbitoides megaliformis* is
470 reported from *Titanosarcolites* bearing strata in Jamaica ranging into the late Maastrichtian (Gunter *et*
471 *al.*, 2002). Consequently, the Guinea Corn Formation and *Titanosarcolites* Beds are considered
472 correlative and assigned a late Maastrichtian age based on the presence of *Chubbina jamaicensis*. The
473 occurrence of *Orbitoides megaliformis* and *Lepidorbitoides* spp. in the Yankee River and Moravia
474 Members of the Guinea Corn Formation suggest moderate water depths and hydrodynamic energy,
475 therefore these two members are interpreted to represent the distal inner ramp close to fair-weather
476 wave base. The interbedded Two Meetings Member may represent a slight oscillation of RSL into
477 shallower water and represent paralic sediments before transgressing back into the deeper waters of the
478 Moravia Member rudist reef. Rare planktonic foraminifera including *Globotruncanella pschadae*,
479 *Globotruncana ventricosa* and *Rugoglobigerina rugosa* in samples from the Two Meetings Member
480 indicate an age no younger than the *Abathomphalus mayaroensis* Zone, which is consistent with the
481 interpretation of the Cretaceous-Tertiary unconformity, where the *Plummerita hantkeninoides*-
482 *Pseudoguembelina hariaensis* Zones are absent.

483 The *Titanosarcolites* beds and Guinea Corn Formation are both interpreted to have been
484 deposited in an inner ramp setting during a transgressive episode following the deposition of marginal
485 marine strata of the *Veniella* shales, Masemure, Slippery Rock and Thomas River Formations,
486 associated with the Ma2 SB. Consequently, the *Titanosarcolites* beds and Guinea Corn Formation
487 represent the transgressive phase of the MTR2 sequence culminating with the Ma2 MFS.

488 The Guinea Corn Formation is overlain by the Summerfield Group in the Central Inlier. The
489 Summerfield Group comprises a massive sandstone polymict conglomerates. These conglomerates
490 occur in repetitive parallel bedded fining upwards sequences between 30 and 60 cm thick. Each of
491 them is floored by conglomerates that fine upwards from cobble to pebble sized polymict clasts that
492 include andesites, mudstones and quartz within a sandstone matrix. The conglomerate fines into coarse
493 and then medium grained sandstones. These conglomerates represent the Mahoe River Formation
494 within the Summerfield Group. Fining upwards successions from basal conglomerate units within the
495 Mahoe River Formation are interpreted to represent fluvial deposits of a braid delta system (Mitchell,
496 2000). This represents a shallowing upwards sequence following deposition of the inner ramp Guinea
497 Corn Formation Limestones. The terrestrially influenced sediments of the Mahoe River Formation
498 represents the culmination of the regressive phase of the MTR2 sequence deposited during a period of
499 RSL lowstand and are interpreted to be associated with the Ma5 SB.

500 The MTR2 sequence is topped by the Cretaceous-Tertiary unconformity (Ma5 to Da1, ca.
501 68.20 to 65.76 Ma), lasting a time span of at least 2.44 Ma. Biostratigraphic analyses indicate that
502 there are no Maastrichtian age sediments younger than the *Abathomphalus mayaroensis* Zone, where
503 the *Plummerita hantkeninoides*-*Pseudoguembelina hariaensis* zones are absent at the Cretaceous-
504 Tertiary unconformity (Fig. 5).

505

506 4.6. Paleocene – Early Eocene (PETR1)

507 The Paleocene to Early Eocene T-R cycle (PETR1) initiates at the Da1 SB (65.76 Ma), reaching
508 average water depths in excess of 100m at the maximum transgressive inflection of the RSL curve
509 correlated to the Da4 MFS (62.23 Ma). The regressive phase of the PETR1 sequence culminates with
510 the Yp9 SB (50.04 Ma) interpreted to correspond to subaerial exposure resulting in the formation of
511 the Early Eocene unconformity (Fig. 6). The PETR1 sequence is represented by Paleocene-Early
512 Eocene age successions of the Blue Mountain Block and Wagwater Trough in the east of Jamaica, and
513 Ecclesdown corehole.

514 The PETR1 sequence initiates with the deposition of the Moore Town Formation which
515 comprises well bedded, dark grey interbedded shales and siltstones in repetitive fining upwards
516 sequences. At the base of each fining upwards package, siltstone beds exhibit bed-parallel cylindrical
517 trace fossils and unidirectional groove structures oriented 030. The siltstones grade normally to
518 parallel and planar shale beds which exhibit internal laminations. The fining upwards siltstone and
519 mudstone packages that exhibit sole structures are interpreted to represent bathyal turbidite deposits.
520 Outer ramp to bathyal water depths are interpreted to have occurred during a period of high RSL,
521 tentatively correlated to the Da4 MFS. The Moore Town Formation is reported to be Danian to
522 Selandian age by Fluegeman (1998). Fluegeman (1998) assigned the Moore Town Formation to
523 micropalaeontological Zones P1c-P3a, and to nannofossil Zones NP4-NP5.

524 The Wagwater Formation stratigraphically overlies the Moore Town Shales. It comprises
525 various lithologies including polymict conglomerates and sandstones with limestone lenses.
526 Limestones contain a fossil assemblage including bivalves, echinoids, ostracods and calcareous,
527 agglutinated and miliolid benthic foraminifera. The foraminifer *Ranikothalia catenula* is observed
528 (Fig. 6). This taxon is described from the Wagwater Formation and is reported to represent a late
529 Paleocene, Thanetian, age (Ramsook and Robinson, 2009). Based on the *Ranikothalia* limestone
530 observed along the Swift River, the Wagwater Formation is assigned an age within the range of
531 micropalaeontological Zones P4b-P5. The Wagwater Formation represents a shallowing upwards,
532 regressive phase of the PETR1 sequence following the deposition of the deep-water turbidites of the
533 Moore Town Formation.

534 The Wagwater Formation is succeeded by the Richmond Formation in the Blue Mountain
535 Block. The Richmond Formation comprises parallel and horizontally bedded fining upwards
536 sequences of medium- to fine-grained sandstones, siltstones and shales. The Richmond Formation
537 contains age-diagnostic palynomorphs including *Diphyes colligerum*, *Homotryblium tenuispinosum*,
538 and *Cyclopsiella 'reticulata'* indicating an age within the range of Middle Eocene, Lutetian to Early
539 Eocene, intra-Ypresian. Consequently, the age of the Richmond Formation is interpreted to be
540 Ypresian. The presence of pyrite and glauconite and iron-rich clay within siliciclastics, suggests
541 deposition in agitated, reducing environments between 50-200m water depth. It is interpreted that the
542 alternating sandstone and shale beds of the Richmond Formation were deposited as fan-delta to
543 submarine-fan deposits as coarse sediments were shed from the highlands of the Blue Mountain Block
544 into prograding deltas encroaching a steep submarine slope (Wescott and Ethridge, 1983).

545 The PETR1 sequence is topped by the Early Eocene unconformity to the east of Jamaica (Yp9
546 to Yp10, ca. 50.04 to 49.58 Ma), lasting a duration of at least 0.46 Ma (Fig. 6).

547

548 4.7. Yellow Limestone Group 1, Ypresian-Lutetian (YTR1)

549 The Yellow Limestone Group of Jamaica is divided into three T-R cycles (YTR1-3). The basal
550 YTR1 cycle initiates at the Yp10 SB (49.58 Ma), reaching average water depths of 15m at the
551 maximum transgressive inflection of the RSL curve correlated to the Lu1 MFS (46.82 Ma). The
552 regressive phase of the YTR1 sequence culminates with the Lu3SB (43.61 Ma). The YTR1 sequence
553 is represented by Early to Middle Eocene age successions (Fig. 6) of predominantly the Clarendon
554 Block of central Jamaica, Content-1/A, Hertford-1 and Pedro Bank-1 wells, and Blowfire Hill
555 corehole.

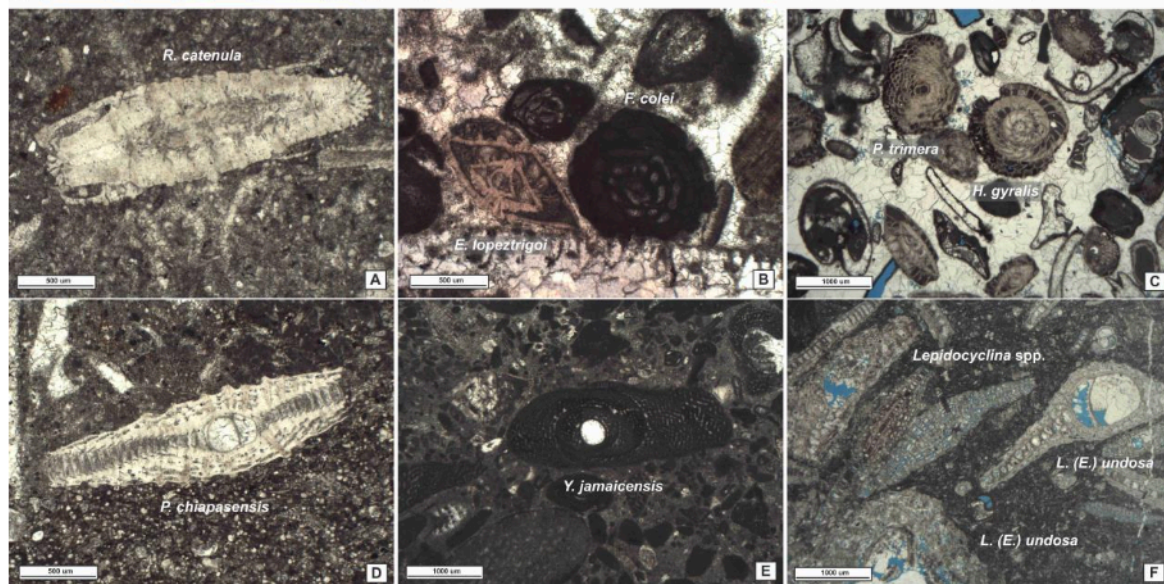
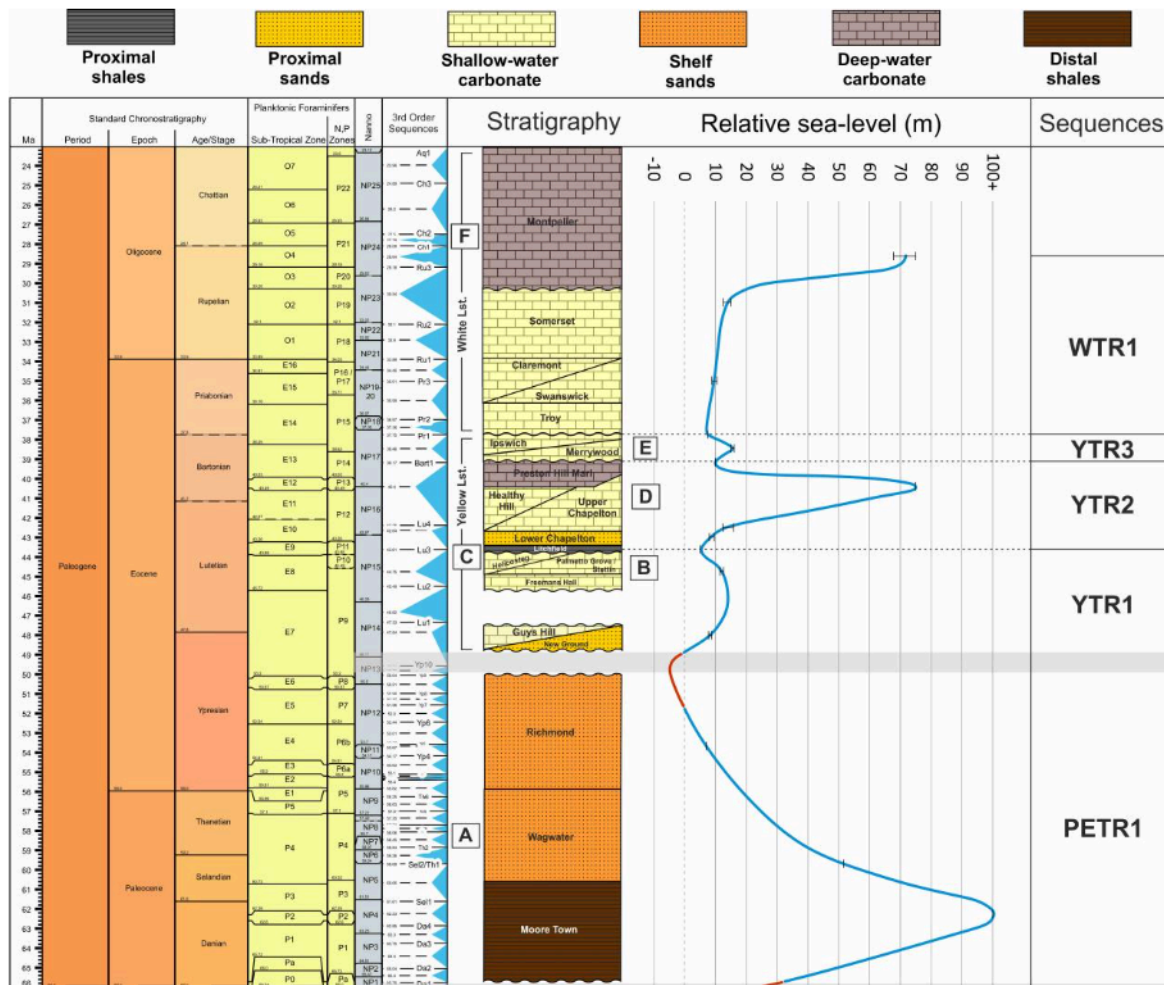
556 The New Ground Formation is here included as a basal unit of the lower Yellow Limestone
557 Group T-R cycle (YTR1). This formation marks the most proximal depositional setting before the
558 transgression of later marine influenced sediments. The New Ground Formation comprises matrix-
559 supported, polymict conglomerates that contain moderately sorted, subangular, low sphericity grains
560 that attain a maximum diameter of 6mm. The matrix consists of a medium grained, texturally and
561 mineralogically immature sandstone. The conglomerate fines upwards to fine-grained sandstone and
562 siltstones that are very well sorted and texturally and mineralogically mature. The fining upwards
563 cycles within the New Ground Formation were laid down in episodes of initial high energy, depositing
564 conglomeratic units and subsequent finer grains as the initial energy was waning. This is interpreted to
565 have been deposited within a fluvial system. The age of this formation is given as Early Eocene by
566 Mitchell *et al.* (2011).

567 The organic-rich Litchfield Formation (Section 4.8) was previously termed the 'Guy's Hill
568 Formation', but subsequently renamed after sediments at the Guy's Hill type locality were found to be

569 Early Eocene in age (Mitchell, 2016). The ‘true’ Guy’s Hill Formation described here refers to
570 sediments similar in appearance to the Litchfield Formation (Section 4.8), but are older and exposed
571 only in a small area close to the town of Guy’s Hill, west of the Benbow Inlier, to the east of the
572 Clarendon Block. The Guy’s Hill Formation comprises well bedded, arkosic sandstones that are coarse
573 to medium-grained, containing well-rounded and well-sorted grains, and occasional lignitic laminae.
574 The sandstones display planar cross bedding, with low angle foresets dipping towards the north. The
575 planar bedded sandstones are overlain by a trough cross-bedded sands that contain climbing foresets
576 which grade upwards into nodular impure limestone. Within this limestone, the presence of the benthic
577 foraminifera *Eoconuloides wellsi* and *Fabularia colei* and the rare occurrence of the planktonic
578 foraminifer *Globanomalina chapmani* constrain the age of the Guy’s Hill Formation to
579 micropalaeontological Zone E4, Ypresian. This is supported by the nannofossil *Discoaster kuepperi*
580 which is assigned to Zones NP14a-NP11, within the Ypresian. The textural immaturity of the
581 siliciclastic components and highly fragmentary nature of the bioclasts within the Guy’s Hill
582 Formation suggests deposition in a proximal, high energy, marine setting. The presence of planar
583 cross-beds may indicate foreshore deposits with seaward inclined laminae directed towards the north.
584 These are overlain by trough cross-bedded, upper shoreface deposits. This suggests a transgressive
585 sequence that deepens upwards towards shallow marine limestones of the overlying Freeman’s Hall
586 and Stettin Formation. The transition from the Guy’s Hill to Freeman’s Hall and Stettin Formations
587 represents the transgressive phase of YTR1 following the Yp10 sequence boundary.

588 The Freeman’s Hall and Stettin Formations consist of irregularly bedded, flaggy limestones
589 that contain a mix of wackestones, packstones and grainstones. These units yield an abundant and
590 diverse fossil assemblage that includes corals, molluscs (including large lucinid bivalves) and large
591 benthic foraminifera. The diverse microfossil assemblage within these limestones (Fig. 6) include the
592 larger benthic foraminifera *Discorinopsis gunteri*, *Fallotella cookei*, *Fabiania cassis*, *Fabularia colei*,
593 *Coskinolina douvillei*, *Fabiania cassis*, *Amphistegina parvula*, *Eoconuloides wellsi*, *Verseyella*
594 *jamaicensis* and *Helicostegina gyralis*, and the planktonic foraminifera *Morozovella crater* which
595 restrict the age of these units to micropalaeontological Zones E8-E9. The assemblage, including
596 common miliolid and agglutinated foraminifera plus significant micrite within packstones and
597 wackestones, indicates deposition within low energy, oligotrophic waters of the proximal inner ramp.
598 The Freeman’s Hall and Stettin Formations are overlain by grainstones dominated by the benthic
599 foraminifera *Helicostegina gyralis*. These *Helicostegina* Beds are constrained to micropaleontological
600 Zone E9 based on the presence *Eoconuloides lopeztrigoi*, *Helicostegina gyralis* and *Pseudolepidina*
601 *trimera* (Fig. 6). The grainstones which contain large amounts of spar, robust lepidocyclinid
602 foraminifera, highly fragmented bioclasts and encrusting coralline red algae indicate high energy
603 depositional setting and may represent a foraminiferal shoal at fair-weather wave base at the distal
604 inner ramp. It is interpreted that the Freemans Hall and Stettin Formations, and *Helicostegina* Beds,

605 were deposited during the transgressive phase of the YTR1 sequence, which culminates with the Lu2
606 MFS. In the Maldon Inlier, the Stettin Formation is unconformably overlain by Litchfield Formation
607 along an unconformity that is interpreted to correspond to the Lu3 SB (Fig. 6).
608



609
 610 Fig. 6 – Jamaican RSL curve of the Paleogene (PETR1, YTR1-3 and WTR1 sequences).
 611 Paleocene limestones of the Wagwater Formation contain rare *Ranikothalia catenula* (A).
 612 Grainstones within the YTR1 sequence contain common *Eoconuloides lopeztrigoi* (B), *Fabularia*

613 *colei* (B), *Pseudolepidina trimera* (C) and *Helicostegina gyralis* (C). The disappearance of the
614 foraminifer *Polylepidina chiapasensis* (D) is characteristic for the top of the Chapelton
615 Formation and YTR2 sequence. The YTR3 sequence is characterised by larger forms of
616 *Yaberinella jamaicensis* (E). Lepidocyclinids increase in abundance and diversity through the
617 upper part of the Yellow Limestone and into the White Limestone Group. Large *Lepidocyclina*
618 (*Eulepidina*) *undosa* (F) characterise the Brown's Town Formation which is often resedimented
619 in calciturbidites of the Montpelier Formation.

620

621 4.8. Yellow Limestone Group 2, Lutetian-Bartonian (YTR2)

622 The second Yellow Limestone Group T-R cycle (YTR2) initiates at the Lu3 SB (43.61 Ma),
623 reaching average water depths of 75m at the maximum transgressive inflection of the RSL curve
624 correlated to the Lu4 MFS (40.40 Ma). The regressive phase of the YTR2 sequence culminates with
625 the Bart1 SB (39.17 Ma). The YTR2 sequence is represented by Middle Eocene age successions (Fig.
626 6) of the Clarendon and Hanover Blocks of western and central Jamaica, Arawak-1, Content-1/A,
627 Negril Spots-1, Pedro Bank-1, Portland Ridge-1 and Santa Cruz-1 wells, and Elderslie and Pindars
628 River-3 coreholes.

629 The Litchfield Formation is found within the Maldon, Marchmont and Central Inliers in the
630 Clarendon Block of Jamaica. This formation contains dark, organic-rich shales and was previously
631 termed the 'Guy's Hill Formation', but subsequently renamed after sediments at the Guy's Hill type
632 locality were found to be Early Eocene in age (Mitchell, 2016). The Litchfield Formation is observed
633 to comprise weakly cemented, porous sandstones and lignite-rich dark mudstones in fining-upwards
634 sequences. In the Maldon Inlier, the Litchfield Formation rests unconformably on top of the Stettin
635 Limestone, where occasionally it slumps into sinkholes developed in the karstic boundary between the
636 two units. The Litchfield Formation is characterised by the presence of high numbers of *Lanagiopollis*
637 *crassa*, which have been documented from the Middle Eocene Avon Park Formation in west central
638 Florida (Jarzen and Dilcher, 2006). A Middle Eocene age is supported by the occurrence of
639 *Margocolporites vanwijhei* and *Monoporites annulatus*, both indicating an age no older than Middle
640 Eocene in the Caribbean region, and *Spinizonocolpites echinatus*, which indicates an age no younger
641 than Eocene (Germeraad *et al.*, 1968). Additionally, the co-occurrence of other taxa such as
642 *Spirosyncolpites spiralis*, *Psilatricolporites caribbiensis*, *Retitricolporites irregularis*,
643 *Spinizonocolpites baculatus*, *Polysphaeridium subtile*, *Homotryblidium* spp. and *Operculodinium* spp. is
644 fully consistent with this age assignment (González-Guzmán, 1967; Jaramillo *et al.*, 2011). The high
645 abundances of the miospore *Lanagiopollis crassa* reflect input from significant developments of
646 mangrove-like vegetation along the adjacent coastline. In tropical areas of West Africa (Gulf of
647 Guinea) and SE Asia (South China Sea), it has been shown that this kind of ecosystems spread during

648 periods of increasing sea level and deposition of lowstand system tracts (Poumot, 1989; Morley,
649 1991). Consequently, it is interpreted that the Litchfield Formation was deposited within a marginal
650 marine, paralic, setting. This supports Robinson and Mitchell's (1999) interpretation that this
651 formation was deposited within a tide-dominated estuarine complex. The Litchfield Formation is
652 interpreted to correspond to a lowstand system tract that deposited during a period of low RSL
653 associated with the Lu3 depositional SB at the base of the YTR2 sequence. The transgressive phase of
654 the YTR2 sequence initiates with paralic and terrestrially-influenced deposits of the Litchfield
655 Formation, transitioning to more marine sediments of the Chapelton Formation.

656 The Chapelton Formation overlies the Litchfield Formation within the Yellow Limestone
657 Group. The Chapelton Formation comprises flaggy limestone containing a diverse fossil assemblage
658 including large bivalves such as *Crassostrea* spp. and *Carolia cantraine* (Trechmann, 1923),
659 gastropods such as *Campanile* spp. and other small molluscan fragments, algae, coral including
660 *Stylophora* spp., and foraminifera. Lepidocyclinid foraminifera are absent from the lower part of the
661 Chapelton Formation but increase in abundance and morphological complexity throughout the
662 Chapelton Limestone succession. The lower part of the Chapelton Formation is constrained to
663 micropalaeontological Zones E9-E10 and contains *Fabularia vaughani/gunteri*, *Verseyella*
664 *jamaicensis* and *Yaberinella hottingeri*. The upper part of the Chapelton Formation is constrained to
665 micropalaeontological Zones E10-E12. This is based on the presence of *Pseudophragmina advena*,
666 *Lepidocyclina (Lepidocyclina) macdonaldi*, *Coleicomus christianaensis*, *Yaberinella jamaicensis* and
667 *Polylepidina chiapasensis* (Fig. 6). The foraminifer *Polylepidina chiapasensis* is diagnostic of the
668 upper Chapelton Formation and its disappearance marks the top of the Chapelton Formation.

669 The Healthy Hill Formation overlies the Chapelton Formation. It comprises a tight, pink-
670 coloured foraminiferal grainstone. The Healthy Hill Formation contains and large miliolids including
671 *Yaberinella jamaicensis* and is dominated by large lepidocyclinid foraminifers including *Eulinderina*
672 spp. and *Polylepidina chiapasensis*. The foraminifer *Polylepidina chiapasensis* is restricted to
673 micropalaeontological Zones E10-E12 therefore the Healthy Hill Formation is assigned a late Lutetian
674 to early Bartonian age. The depositional setting and microfaunal assemblage of the Healthy Hill
675 Formation is similar to the upper Chapelton Formation. It is interpreted that the Healthy Hill
676 Formation represents distal inner ramp deposits that transgress diachronously across the top of the
677 upper Chapelton Formation. This represents the transgressive phase of the YTR2 sequence.

678 The Preston Hill Marl Member of the Font Hill Formation represents a deep water lateral
679 facies transition from the relatively shallower water Chapelton and Healthy Hill Formations. In places,
680 the Preston Hill Marl is observed to transgress across the top of the Chapelton and Healthy Hill
681 Formations. This unit is classified as a planktonic foraminiferal carbonate mudstone and comprises
682 beige-coloured marl, consisting of abundant planktonic foraminifera and echinoid spines visible in
683 hand specimen. The Preston Hill planktonic foraminiferal marl contains abundant carinate planktonic

684 foraminifera including *Morozovelloides* spp. and thick-walled taxa including *Globigerinatheka* spp.
685 These morphologies are indicative of outer ramp to upper bathyal deposits (Bé, 1977). The Preston
686 Hill Marl also contains the planktonic foraminifer *Orbulinoides beckmanni* which is restricted to
687 micropalaeontological Zone E12 and is often found in maximum flooding surface deposits associated
688 with the Lu4 MFS. Consequently, the deposition of the Preston Hill Marl is interpreted to mark the
689 maximum transgressive inflection of the YTR2 sequence corresponding with the Lu4 MFS (Fig. 6).
690 Regression following deposition of the Preston Hill Marl culminated with the formation of the Bart1
691 sequence boundary.

692

693 4.9. Yellow Limestone Group 3, Bartonian-Priabonian (YTR3)

694 The final Yellow Limestone Group T-R cycle (YTR3) initiates at the Bart1 SB (39.17 Ma),
695 reaching average water depths of 15m at the maximum transgressive inflection of the RSL curve
696 correlated to the Bart1 MFS (38.46 Ma). The regressive phase of the YTR3 sequence culminates with
697 the Pr1 SB (37.75 Ma) which separates the Yellow and White Limestone Groups (Fig. 6). The YTR3
698 sequence is represented by latest Middle Eocene age successions of the Clarendon and Hanover
699 Blocks of western and central Jamaica, Arawak-1, Content-1/A, Negril Spots-1, Portland Ridge-1 and
700 Santa Cruz-1 wells.

701 The basal unit of the YTR3 sequence is represented by the Merrywood Formation, an informal
702 name for a lithostratigraphic unit that unconformably overlies the Preston Hill Marl, Healthy Hill and
703 Chapelton Formations. The Merrywood Formation comprises a pale orange to beige-coloured
704 foraminiferal packstone containing a large amount of micrite. This formation contains abundant
705 miliolids including large specimens of *Yaberinella jamaicensis* and *Fabularia hanzawai*. The
706 Merrywood Formation is constrained to micropalaeontological Zones E13-E14, based on the highest
707 occurrences of *Fabularia vaughani/gunteri* and *Cushmania americana* and the presence of *Fabularia*
708 *hanzawai* which is restricted to these two biozones. The large number of miliolids and agglutinated
709 foraminifera, together with a large amount of micrite matrix, indicates this unit was deposited in the
710 low energy, oligotrophic waters of the proximal inner ramp. Continued transgression resulted in the
711 deposition of the overlying distal inner ramp deposits of the Ipswich Formation within the YTR3
712 sequence.

713 The Ipswich Formation is the uppermost unit of the Yellow Limestone Group and is
714 unconformably overlain by the White Limestone Group. The Ipswich Formation is observed to
715 comprise a grey coloured foraminiferal mud-lean packstone to grainstone. This unit is dominated by
716 an abundant and diverse lepidocyclinid assemblage including *Lepidocyclina (Lepidocyclina)*
717 *macdonaldi*, *L. (L.) pustulosa* and *L. (L.) ariana*, although it also contains echinoid plates and rare
718 specimens of large *Yaberinella jamaicensis*. The presence of *Fabularia hanzawai*, *Polylepidina*

719 *proteiformis* and *Lepidocyclina (Lepidocyclina) macdonaldi* restrict the age of the Ipswich Formation
720 to micropalaeontological Zones E13-E14. The presence of *Lepidocyclina (Lepidocyclina) ariana* in
721 some samples is restricted to Zone E13. The dominance of lepidocyclinids and large amount of calcite
722 spar within these grainstones indicate it was deposited in an energetic environment such as a
723 foraminiferal shoal and/or at fair weather wave base at the distal inner ramp. This represents a minor
724 deepening trend following on from the proximal inner ramp deposits of the Merrywood Formation.
725 This deepening trend marks the transgressive phase of the YTR3 sequence, culminating with the Bart1
726 MFS. Subsequent regression terminates at the Pr1 depositional SB and base of the overlying White
727 Limestone Group (Fig. 6).

728

729 4.10. *White Limestone Group, Priabonian-Rupelian (WTR1)*

730 The White Limestone Group T-R cycle (WTR1) initiates at the Pr1 SB (37.75 Ma), reaching
731 average water depths of approximately 75m at the maximum transgressive inflection of the RSL curve
732 correlated to the Ru3 MFS (28.64 Ma). The WTR1 sequence is represented by Late Eocene-Oligocene
733 age successions (Fig. 6) of Jamaica, Arawak-1, Negril Spots-1, Pedro Bank-1, Portland Ridge-1 and
734 Santa Cruz-1 wells, and Ecclesdown corehole.

735 The Troy Formation unconformably overlies the Yellow Limestone Group and is the basal unit
736 of the White Limestone. It comprises a dolomitic limestone that is black in colour on its weathered
737 surface and pale orange/beige in colour on its fresh surface. Samples from the Troy Formation display
738 pervasive dolomitisation with loss of original fabric; however rare exceptions retain ‘ghosts’ of larger
739 benthonic foraminifera. Consequently, samples analysed for biostratigraphy yielded poor results due to
740 the presence of pervasive dolomitisation. However, due to the Troy Formation’s stratigraphic position
741 between two well constrained units (the Ipswich and Swanswick Formations) it is assigned to
742 micropalaeontological Zone E14. ‘Ghosts’ of conical dictyoconids and presumed abundance of fine-
743 grained micrite prior to dolomitisation suggest the Troy Formation was deposited within very shallow,
744 low energy, oligotrophic waters of the proximal inner ramp during a period of low RSL associated
745 with the Pr1 depositional SB.

746 The Swanswick and Claremont Formations overlie the Troy Formation within the White
747 Limestone Group succession. These units are observed to comprise massive, white coloured bioclastic
748 grainstone. They contain an abundant and diverse foraminiferal assemblage dominated by the small
749 rotaliid *Neorotalia mexicana* and large morphologically advanced lepidocyclinids. The presence of
750 *Lepidocyclina (Nephrolepidina) yurnagunensis* within the Swanswick Formation indicates an age no
751 older the Zone E16. Consequently, the Swanswick Formation is assigned a Late Eocene, late
752 Priabonian, age and continues the deepening upwards, transgressive trend of the WTR1 sequence
753 transitioning from the proximal inner ramp deposits of the Troy Formation. The presence of large platy

754 lepidocyclinids, encrusting red algae and grainstone facies suggest that the Swanswick and Claremont
755 Formations were deposited in a distal inner ramp setting at fair-weather wave base where high
756 hydrodynamic energy favours the precipitation of coarse calcite spar.

757 The Swanswick and Claremont Formations are overlain by the Montpelier Formation, an
758 extremely thick and widespread unit found across most of Jamaica. The Montpelier Formation
759 comprises interbedded chalk and chert, interpreted to represent deep-water calciturbidites deposited
760 above the Calcite Compensation Depth (CCD). However, these turbidites must have been deposited a
761 short distance from the shelf such as to receive transported (allochthonous) shallow water taxa
762 including *Lepidocyclina* (*Lepidocyclina*) *cannellei*, *Lepidocyclina* (*Eulepidina*) *undosa*, *Heterostegina*
763 *antillea* and *Miogypsinoides* spp., sourced from the contemporaneous Brown's Town Formation that
764 was deposited upslope of the Montpelier Formation. The presence of *Lepidocyclina* (*Lepidocyclina*)
765 *cannellei*, *Lepidocyclina* (*Nephrolepidina*) *yurnagunensis*, *Heterostegina antillea* and *Nummulites*
766 *fichteli* in samples from the Montpelier Formation constrain this unit to Zones O3-O5. These biozones
767 represent the 'late' Rupelian and 'early' Chattian stages of the Oligocene. The presence of the
768 foraminifera *Lepidocyclina* (*Nephrolepidina*) *yurnagunensis*, *Heterostegina antillea*, *Nummulites*
769 *fichteli*, *Lepidocyclina* (*Lepidocyclina*) *cannellei*, *Lepidocyclina* (*Eulepidina*) *undosa* (Fig. 6) within the
770 Brown's Town Formation are also restricted to the Oligocene, micropalaeontological Zone O5. This
771 corroborates the age of the transported units within the calciturbidites observed within the Montpelier
772 Formation. The deposition of the Montpelier Formation is associated with the Ru3 MFS and marks
773 the culmination of the WTR1 transgressive sequence that initiated at the Pr1 sequence boundary with
774 the deposition of the Troy Formation (Fig. 6).

775

776 5. Discussion

777 5.1. The Jamaican relative sea-level curve

778 Transgressive-regressive cycles identified within the Jamaican sea-level curve represent second (10^7
779 years) to fourth (10^5 years) order sequences, although most tie to globally recognised third order (10^6
780 years) sequences of Hardenbol et al., (1998). The EKTR1 and PETR1 sequences are regarded as
781 second order sequences, lasting a duration of approximately 23 Ma and 16 Ma, respectively. The
782 duration of these sequences is consistent with long term regional tectonic events including the
783 assembly of CLIP fragments and back/fore-arc spreading in the 'middle' Cretaceous and Late
784 Cretaceous to Paleogene rifting across the Nicaragua Rise (see Section 2). The STR1 (ca. 4 Ma),
785 CTR1 (ca. 7.5 Ma), MTR1 (ca. 3 Ma), YTR1 (ca. 5.5 Ma), YTR2 (ca. 4.5 Ma) and WTR1 (ca. 9.25
786 Ma) depositional cycles represent third order sequences and are regarded to be controlled by global
787 eustatic trends (see Section 5.2). The MTR2 (ca. 1 Ma) and YTR3 (ca. 1.25 Ma) may represent fourth
788 order sequences where local tectonism dictates shifts in facies.

789 In carbonate dominated sequences of the Maastrichtian, and Paleogene Yellow and White
790 Limestone groups the average rates of RSL rise are calculated as approximately 26.6 m/Ma for MTR1,
791 10 m/Ma for MTR2, 3.6 m/Ma for YTR1, 15.5 m/Ma for YTR2, 4 m/Ma for YTR3 and 7 m/Ma for
792 WTR1. Given the lowest accumulation rates of prograding carbonates is regarded as 30 m/Ma
793 (Schlager, 1981; Handford and Loucks, 1993; Wissler *et al.*, 2003), production rates of Maastrichtian
794 and Paleogene carbonates could sufficiently keep pace with the low rates of RSL rise calculated for
795 these sequences. This accounts for the several kilometres thick carbonate successions of Maastrichtian
796 and Paleogene age units observed in Jamaica. However, the sharp change in gradient in the WTR1
797 sequence in the late Rupelian is calculated to require an increase in the rate of RSL rise to 27.5 m/Ma.
798 Although optimal carbonate accumulation rates should keep pace with this rate of RSL rise, Jamaican
799 carbonate platforms nevertheless succumbed to drowning during the Oligo-Miocene evident by thick
800 sequences of the deep-water Montpelier Formation overlying shallow platform carbonates across the
801 island. It is therefore interpreted that environmental factors (e.g. Mutti *et al.*, 2005) exerted a greater
802 control than global eustasy later on during the WTR1 sequence.

803 The curve presented here constitutes a simplified first attempt at reconstructing RSL change in
804 Jamaica. This curve may be refined in the future by higher resolution field sampling, well analyses and
805 numerical forward modelling. This will enable the identification of further fourth and even fifth order
806 depositional cycles and better determine the, potentially multiple, controls on deposition of these
807 sequences.

808

809 5.2. *Comparisons with global sea-level curves*

810 Maximum transgressive and regressive inflections of the Jamaican RSL curve correlate with
811 similar trends in global sea-level curves of Haq and Al-Qahtani (2005), Kominz *et al.* (2008), Snedden
812 and Liu (2010) and Miller *et al.* (2005; 2011), however they do not resemble those of Müller *et al.*
813 (2008). Major unconformities in Jamaica are particularly well correlated to significant events of global
814 sea-level fall (Fig. 7). However, this coincidence is unsurprising as many of the unconformities are
815 interpreted to have formed subaerially, during periods of collisional uplift which, if occurring at the
816 same time as global eustatic sea-level fall, will result in the formation of substantial unconformities
817 lasting a time span of several million years. Many of the T-R cycles initiate during a period of low
818 RSL, attributed to tectonic uplift, and are followed by transgressive episodes influenced by global
819 eustasy or regional subsidence.

820 The Turonian-Coniacian unconformity between the EKTR1 and STR1 sequences coincides with
821 a sharp decrease in the short-term trend of mean global sea-level recognised by Haq and Al-Qahtani
822 (2005) and Snedden and Liu (2010) who record a drop in sea-level with a magnitude of approximately
823 50m and 110m, respectively (Fig. 7). Both Haq and Al-Qahtani (2005) and Snedden and Liu (2010)

824 also record a sharp increase in sea-level shortly after; with maximum transgressive inflections of the
825 short-term mean sea-level trend coinciding with that of the STR1 sequence (Fig. 7).
826

828 **Fig. 7 – The Jamaican RSL curve compared to global mean sea-level curves of Haq and Al-**
829 **Qahtani (2005), Kominz *et al.* (2008) Muller *et al.* (2008), Snedden and Liu (2010) and Miller**
830 **(2005; 2011). Major Jamaican unconformities correlate with periods of significant global mean**
831 **sea-level fall, the duration of the unconformities are approximately equal to the wave-length of**
832 **sea-level fall.**

833

834 The early Campanian unconformity between the STR1 and CTR1 sequences also coincides
835 with a decrease in global mean sea-level recorded by Haq and Al-Qahtani (2005), Kominz *et al.*
836 (2008), Snedden and Liu (2010) and Miller *et al.* (2005; 2011) of a magnitude between approximately
837 20m and 60m (Fig. 7). The Campanian-Maastrichtian unconformity between the CTR1 and MTR1
838 sequences correlates with a drop in mean global sea-level of approximately 60m recorded by Haq and
839 Al-Qahtani (2005) and Snedden and Liu (2010). The maximum transgressive inflection of the MTR1
840 sequence correlates to a period of high mean global sea-level recorded as 285m above present day by
841 Haq and Al-Qahtani (2005).

842 The Cretaceous-Tertiary unconformity between the MTR2 and PETR1 sequences coincides
843 with a decrease in global mean sea-level recorded by Haq and Al-Qahtani (2005), Kominz *et al.*
844 (2008), Snedden and Liu (2010) and Miller *et al.* (2005; 2011) of a magnitude between approximately
845 20m and 40m (Fig. 7). Following the Cretaceous-Tertiary unconformity, the PETR1 sequence does not
846 fit global mean sea level trends of RSL fall due to the Late Cretaceous to Paleogene rifting event
847 which occurred across the Nicaragua Rise (Mitchell, 2003) resulting in tectonic subsidence and
848 localised RSL rise in Jamaica. The Early Eocene unconformity between the PETR1 and YTR1
849 sequences also coincides with a significant drop in the short-term mean global sea-level trend of
850 between 60m and 110m recorded by Haq and Al-Qahtani (2005) and Snedden and Liu (2010). Minor
851 oscillations in the Jamaican RSL curve within the Yellow Limestone Group correlate with minor
852 oscillations in the short-term sea-level trend of Haq and Al-Qahtani (2005). The maximum
853 transgressive inflections of the YTR2 and WTR1 sequences coincide with significant maximum
854 transgressive inflections of the short-term mean global sea-level curves of Haq and Al-Qahtani (2005),
855 Kominz *et al.* (2008) and Snedden and Liu (2010), although environmental deterioration may play a
856 greater role towards the end of the latter sequence (e.g. Mutti *et al.*, 2005).

857 The duration of the major Jamaican unconformities are approximately equal to the wavelength
858 of periods of mean global sea-level fall (Fig. 7). The Turonian-Coniacian unconformity is calculated
859 by this study to last 2.39 Ma, while the wavelength of sea-level fall at this time in the Haq and Al-
860 Qahtani (2005) curve lasts approximately 2.7 Ma. The early Campanian unconformity lasts 2.55 Ma in
861 this study, the wavelength in the Miller *et al.* (2005; 2011) curves lasts approximately 2.6 Ma. The
862 Campanian-Maastrichtian unconformity lasts 1.86 Ma in this study where the wavelength of the
863 Snedden and Liu (2010) curve lasts 2.6 Ma. The Cretaceous-Tertiary unconformity lasts 2.44 Ma and

864 the wavelength of the Kominz et al. (2008) curve lasts 2.9 Ma. Finally, the Early Eocene unconformity
865 is calculated as 0.46 Ma by this study, whereas wavelengths of the Snedden and Liu (2010) and Haq
866 and Al-Qahtani (2005) curves last 1.6 Ma and 2.2 Ma, respectively.

867

868 **6. Conclusions**

869 The ten Jamaican T-R sequences identified by this study each correspond to one complete
870 cycle of RSL rise and fall. Comparisons of the Jamaican RSL curve with global trends show that local
871 tectonism exerts a significant control on the deposition of sedimentary sequences in Jamaica. This is
872 most evident where several unconformities attributed to major tectonic episodes also coincide with
873 significant falls in mean global sea-level. The duration of the unconformities in Jamaica is comparable
874 to the wavelength in oscillations of the short-term global trends of Haq and Al-Qahtani (2005) and
875 Snedden and Liu (2010). Following major tectonic episodes, the Jamaican RSL curve follows global
876 eustatic trends. The amplitudes of mean global sea-level rise and fall also match the amplitude of
877 transgressive and regressive phases identified in Jamaica, in the order of several tens of metres. The
878 relatively low rates of RSL rise and fall calculated in Jamaica and thick successions of carbonate
879 sequences suggest that carbonate production rates were able to respond adequately to gradual changes
880 in RSL during the Cretaceous to Paleogene until succumbing to drowning during a sharp increase in
881 the rate of RSL rise and environmental deterioration in the Oligo-Miocene.

882

883 **Acknowledgments**

884 The authors would like to thank CGG for funding this research and the Petroleum Corporation of
885 Jamaica for providing samples and assistance during fieldwork and continued support throughout the
886 study. We would also like to thank Prof. Simon Mitchell and the University of West Indies for
887 assistance in the field. Finally, we would like to credit CGG NPA Satellite Mapping for the creation of
888 the geological map in Figure 1.

889

890 **Funding**

891 This research was funded by CGG.

892

893 Declaration of interest: None

894 **References**

- 895 Abbott Jr, R.N., Bandy, B.R. and Rajkumar, A., 2013. Cenozoic burial metamorphism in eastern
896 Jamaica. *Caribbean Journal of Earth Science*, 46, pp.13-30.
897
- 898 Aguilar, M., Bernaus, J.M., Caus, E. and Hottinger, L., 2002. *Lepidorbitoides minima* Douvillé from
899 Mexico, a foraminiferal index fossil for the Campanian. *J. Foramin. Res.*, v. 32, no. 2, p.126-134.
900
- 901 Arden, D.D., Jr., 1969. Geologic history of the Nicaraguan Rise. *Trans. Gulf Coast Assoc. Geol. Soc.*,
902 v. 19, p. 295-309.
903
- 904 Arden, D.D., Jr., 1977. Geology of Jamaica and the Nicaragua Rise. In: Nairn, A.E.M., Stehli, F.G.
905 and Brown, G.M. (eds.), *The ocean basins and margins (Volume 3): the Gulf of Mexico and the*
906 *Caribbean*. *Geophysical Journal of the Royal Astronomical Society*, v. 48, no. 1, p.617-661.
907
- 908 Baker, R.D., Hallock, P., Moses, E.F., Williams, D.A. and Ramirez, A., 2009. Larger foraminifers of
909 the Florida reef tract, USA: Distribution patterns on reef-rubble habitats. *J. Foramin. Res.*, v. 39, no. 4,
910 p. 267-277.
911
- 912 Bé, A.W.H., 1977 An ecological, zoogeographic and taxonomic review of Recent planktonic
913 foraminifera. In: Ramsey, A.T.S (ed.) *Oceanic micropalaeontology*, p.1-100. Academic Press, London.
914
- 915 Beavington-Penney, S.J. and Racey, A., 2004. Ecology of extant nummulitids and other larger benthic
916 foraminifera: applications in palaeoenvironmental analysis. *Earth-Science Reviews*, v. 67, p. 219-265.
917
- 918 Benton, M.J. and Harper, D.A.T., 1997. *Basic palaeontology*. Harlow: Addison Wesley Longman.
919 342pp.
920
- 921 Berggren, W.A. and Pearson, P.N., 2005. A revised (sub)tropical planktonic foraminiferal zonation of
922 the Eocene and Oligocene. *J. Foramin. Res.*, v. 35, p. 279-298.
923
- 924 Berggren, W.A., Kent, D.V., Swisher, C.C. III and Aubry, M-P., 1995. A revised Cenozoic
925 geochronology and chronostratigraphy. In: Berggren, W.A., Kent, D.V., Aubry M-P and Hardenbol, J.
926 (eds.), *Geochronology, time scales and global stratigraphic correlation*. *SEPM (Soc. Sed. Geol.)*, Spec.
927 *Publ.*, no. 54, p. 129-212.
928

929 BouDagher-Fadel, M.K., 2008. Evolution and geological significance of larger benthic foraminifera.
930 Developments in palaeontology and stratigraphy, v. 21, Elsevier, 539pp.
931
932 Brown, I. and Mitchell, S.F., 2010. Lithostratigraphy of the Cretaceous succession in the Benbow
933 Inlier, Jamaica. Caribbean Journal of Earth Science, v. 41, no. 2, p. 25-37.
934
935 Brown, N.K. and Bronnimann, P., 1957. Some Upper Cretaceous rotaliids from the Caribbean region.
936 Micropaleontology, p. 29-38.
937
938 Burchette, T.P. and Wright, V.P., 1992. Carbonate ramp depositional systems. Sediment. Geol., v. 79,
939 no. 1, p. 3-57.
940
941 Burke, K., Fox, P.J. and Şengör, A.M.C., 1978. Buoyant ocean floor and the evolution of the
942 Caribbean. *Journal of Geophysical Research: Solid Earth*, 83(B8), pp.3949-3954.
943
944 Burke, K., 1988. Tectonic evolution of the Caribbean. Annual Reviews of Earth and Planetary
945 Science, 16, 201-230.
946
947 Cochran, W.J., Spotila, J.A., Prince, P.S. and McAleer, R.J., 2017. Rapid exhumation of Cretaceous
948 arc-rocks along the Blue Mountains restraining bend of the Enriquillo-Plantain Garden fault, Jamaica,
949 using thermochronometry from multiple closure systems. Tectonophysics, 721, 292-309.
950
951 DeMets, C. and Wiggins-Grandison, M., 2007. Deformation of Jamaica and motion of the Gonave
952 microplate from GPS and seismic data. *Geophysical Journal International*, 168(1), pp.362-378.
953
954 Droxler, A., Cunningham, A., Hine, A.C., Hallock, P., Duncan, D., Rosencrantz, E., Buffler, R. and
955 Robinson, E., 1993. Late middle Miocene Segmentation of an Eocene-early Miocene carbonate
956 megabank on the Northern Nicaragua Rise tied to the tectonic activity at the North America/Caribbean
957 plate boundary zone. AAPG Bulletin, v. 77.
958
959 Droxler, A., Morse, J.W., Glaser, K.S., Haddad, G.A. and Baker, P.A., 1991. Surface sediment
960 carbonate mineralogy and water column chemistry: Nicaragua Rise versus the Bahamas. Marine
961 geology, v. 100, no. 1-4, p.277-289.
962

963 Eva, A.N., 1976. The palaeoecology and sedimentology of Middle Eocene larger foraminifera in
964 Jamaica. 1st. Int. Symp. on benthonic foraminifera of continental margins, Part B. Paleoecology and
965 Biostratigraphy, Maritime Sediments, Spec. Pub., v. 1, p. 467-475.
966

967 Fluegeman, R.H., 1998. Planktonic and benthic foraminifera from the Moore Town Shales (Paleocene)
968 at the Fellowship Bridge section, Portland, Jamaica. In: Caribbean Geology: Into the 3rd Millennium:
969 Transactions of the 15th Caribbean Geological Conference, 29th June-2nd July, p. 149-154.
970

971 Germeraad, J.H., Hopping, C.A., and Muller, J., 1968. Palynology of Tertiary sediments from tropical
972 areas. *Review of Palaeobotany and Palynology*, 6: 189–348.
973

974 Gonzalez-Guzman, A.E., 1967. A palynological study on the upper Los Cuervos and Mirador
975 formations (Lower and middle Eocene; Tibu area, Colombia). Brill, Leiden 129 p.
976

977 Gradstein, F.M., Ogg, J.G., Schmitz M.D. and Ogg, G.M., 2012. The Geologic Time Scale 2012.
978 Elsevier, Amsterdam, v.1-2, p. 1-1144.
979

980 Grippi, J., 1978. Geology of the Lucea Inlier, western Jamaica. PhD thesis
981

982 Gunter, G.C., Robinson, E. and Mitchell, S.F., 2002. A new species of *Omphalocyclus*
983 (Foraminiferida) from the Upper Cretaceous of Jamaica and its stratigraphical significance. *Journal of*
984 *Micropalaeontology*, 21(2), pp.149-153.
985

986 Handford C.R. and Loucks, R.G., 1993. Carbonate depositional sequences and systems tracts—
987 responses of carbonate platforms to relative sea-level changes. In: Loucks RG, Sarg JF (eds)
988 Carbonate sequence stratigraphy, vol 57. American Association of Petroleum Geologists, Memoir,
989 Tulsa, pp 3–41
990

991 Hanzawa, S., 1962. Upper Cretaceous and Tertiary three-layered larger foraminifera and their allied
992 forms. *Micropaleontology*, pp.129-186.
993

994 Hallock, P. and Glenn, E.C., 1986. Larger foraminifera: A tool for paleoenvironmental analysis of
995 Cenozoic carbonate depositional facies. *Palaios*, v. 1, p. 55-64.
996

997 Haq, B.U., Al-Qahtani, A.M., 2005. Phanerozoic cycles of sea-level change on the Arabian Platform.
998 *GeoArabia* 10 (2), 127-160.

999
1000 Hardenbol, J., Thierry, J., Farley, M.B., Jacquin, T., De Graciansky, P-C. and Vail, P.R., 1998.
1001 Mesozoic and Cenozoic sequence chronostratigraphic framework of European basins. In: de
1002 Graciansky, P-C. *et al.* (eds.), Mesozoic and Cenozoic sequence stratigraphy of European basins.
1003 SEPM Spec. Publ., no. 61, p. 109-127.
1004
1005 Hastie, A.R., Kerr, A.C., McDonald, I., Mitchell, S.F., Pearce, J.A., Wolstencroft, M. and Millar, I.L.,
1006 2010a. Do Cenozoic analogues support a plate tectonic origin for Earth's earliest continental crust?
1007 *Geology*, v. 38, p. 495–498.
1008
1009 Hastie, A.R., Kerr, A.C., McDonald, I., Mitchell, S.F., Pearce, J.A., Millar, I.L., Barfod, D. and Mark,
1010 D.F., 2010b. Geochronology, geochemistry and petrogenesis of rhyodacite lavas in eastern Jamaica: A
1011 new adakite subgroup analogous to early Archaean continental crust? *Chemical Geology*, v. 276, p.
1012 344-359.
1013
1014 Hastie, A.R., Mitchell, S.F., Kerr, A.C., Minifie, M.J., and Millar, I.L., 2011. Geochemistry of rare
1015 high-Nb basalt lavas: Are they derived from a mantle wedge metasomatised by slab melts?
1016 *Geochimica et Cosmochimica Acta*, v. 75, p. 5049-5072.
1017
1018 Hohenegger, J., 2005. Estimation of environmental paleogradient values based on presence/absence
1019 data: a case study using benthic foraminifera for paleodepth estimation. *Palaeogeography,*
1020 *Palaeoclimatology, Palaeoecology*, v. 217, p. 115-130.
1021
1022 Jackson, T.A., 1987. The petrology of Jamaican Cretaceous and Tertiary volcanic rocks and their
1023 tectonic significance. *Proceedings of a workshop on the status of Jamaican geology: Geological*
1024 *Society of Jamaica, special issue*, p. 107-119.
1025
1026 Jaramillo, C., Rueda, M., Torres, V., 2011. A palynological zonation for the Cenozoic of the Llanos
1027 and Llanos Foothills of Colombia. *Palynology*, 35(1): 46–84.
1028
1029 Jarzen, D.M. and Dilcher, D.L., 2006. Middle Eocene terrestrial palynomorphs from the Dolime
1030 Minerals and Gulf Hammock Quarries, Florida, USA. *Palynology*, v. 30, no. 1, p. 89-110.
1031
1032 Jiang, M.,J. and Robinson, E., 1987. Calcareous nannofossils and larger foraminifera in Jamaican
1033 rocks of Cretaceous to early Eocene age. *Status of Jamaican Geology*, p. 24-51
1034

- 1035 Katz, M.E. and Miller, K.G., 1993. Miocene-Pliocene bathyal benthic foraminifera and the uplift of
1036 Buff Bay, Jamaica. *Geological Society of America Memoirs*, 182, pp.219-254.
- 1037
- 1038 Kauffman, E.G. and Sohl, N.F., 1974. *Structure and evolution of Antillean Cretaceous rudist*
1039 *frameworks*. Verh. Nat. Forsch. Ges. Basel, 84/1: 339-467.
- 1040
- 1041 Kerr, A.C., White, R.V., Thompson, P.M. E., Tarney, J., Saunders, A.D., 2004. No oceanic plateau—
1042 no Caribbean plate? The seminal role of an oceanic plateau in Caribbean plate evolution. In: Bartolini,
1043 C., Buffler, R.T., Blickwede, J. (eds.). *The Circum-Gulf of Mexico and the Caribbean: Hydrocarbon*
1044 *habitats, basin formation, and plate tectonics*. American Association of Petroleum Geologists Memoir
1045 79, 126–168.
- 1046
- 1047 Kirby, M.X. and Saul, L.R., 1995. The Tethyan bivalve *Roudairia* from the Upper Cretaceous of
1048 California. *Palaeontology*, v. 38, no. 1, p.23-38.
- 1049
- 1050 Kominz, M.A., K.G. Miller, and J.V. Browning. 1998. Long-term and short-term global Cenozoic sea-
1051 level estimates. *Geology* 26:311–314.
- 1052
- 1053 Krijnen, J.P., Macgillavry, H.J. and Van Dommelen, H., 1993. Review of Upper Cretaceous orbitoidal
1054 larger foraminifera from Jamaica, West Indies, and their connection with rudist assemblages.
1055 *Geological Society of America Memoirs*, v. 182, p.29-64.
- 1056
- 1057 Kumar, A. and Grambast-Fessard, N., 1984. Maastrichtian charophyte gyrogonites from Jamaica.
1058 *Micropaleontology*, v. 30, no. 3, p. 263-267.
- 1059
- 1060 Kumar, A. and Oliver, R., 1984. The occurrence and geological significance of charophyte
1061 gyrogonites from the Slippery Rock Formation (Maastrichtian), Central Inlier, Jamaica. *Caribbean*
1062 *Journal of Science*, v. 20, p. 29-34.
- 1063
- 1064 Lewis, J.F., Kysar Mattiotti, G., Perfit, M. and Kamenov, G., 2011. Geochemistry and petrology of
1065 three granitoid rock cores from the Nicaraguan Rise, Caribbean Sea: implications for its composition,
1066 structure and tectonic evolution. *Geologica Acta: an international earth science journal*, 9(3-4).
- 1067
- 1068 Mann, P., Draper, G. and Burke, K. 1985. Neotectonics of a strike-slip restraining bend system,
1069 Jamaica. In: K. Biddle and N. Christie-Blick (Eds.), *Strike-slip deformation, basin formation, and*
1070 *sedimentation*. *SEPM Special Issue*, 37, 211-226.

1071
1072 Mann, P., Taylor, F.W., Lawrence Edwards, R. and Ku, T-L., 1995. Actively evolving microplate
1073 formation by oblique collision and sideways motion along strike-slip faults: an example from the
1074 northeastern Caribbean plate margin. *Tectonophys.*, v.246, p.1-69.
1075
1076 Martini, E., 1971. Standard Tertiary and Quaternary calcareous nannoplankton zonation. Proc. 2nd
1077 Planktonic Conf., Roma, 1969, v. 2, p. 739-785.
1078
1079 Miller, K.G., M.A. Kominz, J.V. Browning, J.D. Wright, G.S. Mountain, M.E. Katz, P.J. Sugarman,
1080 B.S. Cramer, N. Christie- Blick, and S.F. Pekar. 2005. The Phanerozoic record of global sea-level
1081 change. *Science* 310:1,293–1,298.
1082
1083 Miller, K.G., Mountain, G.S., Wright, J.D., Browning, J.V., 2011. A 180-million-year record of sea
1084 level and ice volume variations from continental margin and deep-sea isotopic records. *Oceanography*
1085 24 (2), 40-53
1086
1087 Mitchell, S.F., 2000. SS03 Facies analysis of a Cretaceous-Paleocene volcanoclastic braid-delta. GSTT
1088 2000 SPE conference proceedings, 1-9.
1089
1090 Mitchell, S.F., 2003. Sedimentary and tectonic evolution of central Jamaica. In: Bartolini, C., Buffler,
1091 R.T. and Blickwede, J.F. (eds.) *The Circum-Gulf of Mexico and the Caribbean: hydrocarbon habitats,*
1092 *basin formation, and plate tectonics.* AAPG Memoir, v. 79, Tulsa, Arizona, USA, p. 605-623.
1093
1094 Mitchell, S.F., 2005. Biostratigraphy of Late Maastrichtian larger foraminifers in Jamaica and the
1095 importance of Chubbina as a Late Maastrichtian index fossil. *Journal of Micropalaeontology*, v. 24,
1096 no. 2, p.123-130.
1097
1098 Mitchell, S.F., 2006. Timing and implications of Late Cretaceous tectonic and sedimentary events in
1099 Jamaica. *Geologica Acta: an international earth science journal*, 4(1-2).
1100
1101 Mitchell, S.F., 2013. The lithostratigraphy of the Central Inlier, Jamaica. *Caribbean Journal of Earth*
1102 *Science*, v. 46, p. 31-42.
1103
1104 Mitchell, S.F., 2016. Geology of the western margin of the Benbow Inlier-implications for the
1105 relationship between the Yellow Limestone and White Limestone groups (with the description of the
1106 Litchfield Formation, new name). *Caribbean Journal of Earth Science*, v. 48, p. 19-25.

1107
1108 Mitchell, S.F. and Blissett, D., 2001. Lithostratigraphy of the late Cretaceous to ?Paleocene succession
1109 in the western part of the Central Inlier of Jamaica. *Caribbean Journal of Earth Science*, 35, 19-31.
1110
1111 Mitchell, S.F. and Ramsook, R., 2009. Rudist bivalve assemblages from the Back Rio Grande
1112 Formation (Cretaceous: Campanian) of Jamaica and their stratigraphic significance. *Cretaceous*
1113 *Research*, v. 30, no. 2, p.307-321.
1114
1115 Mitchell, S.F. and Edwards, T.C.P., 2016. Geology of the Maastrichtian (Upper Cretaceous)
1116 succession of the Jerusalem Mountain Inlier in western Jamaica. *Caribbean Journal of Earth Science*,
1117 48, 29-36.
1118
1119 Mitchell, S.F., Ramsook, R., Coutou, R. and Fisher, J., 2011. Lithostratigraphy and age of the St.
1120 Ann's Great River Inlier, northern Jamaica. *Caribbean Journal of Earth Science*, v. 42, p. 1-16.
1121
1122 Morley, R.J., 1991. Tertiary stratigraphic palynology in Southeast Asia: current status and new
1123 directions. *Geological Society of Malaysia Bulletin*, 28: 1–36.
1124
1125 Müller, R.D., Sdrolias, M., Gaina, C., Steinberger, B., Heine, C., 2008. Long-term sealevel
1126 fluctuations driven by ocean basin dynamics. *Science* 319, 1357-1362.
1127
1128 Murray, J.W., 1991. Ecology and palaeoecology of benthic foraminifera. Longman Group UK Ltd.
1129 397pp.
1130
1131 Murray, J.W., 2006. Ecology and applications of benthonic foraminifera. Cambridge University Press,
1132 426pp.
1133
1134 Mutti, M., Drozler, A.W. and Cunningham, A.D., 2005. Evolution of the Northern Nicaragua Rise
1135 during the Oligocene–Miocene: drowning by environmental factors. *Sedimentary Geology*, v. 175, no.
1136 1, p. 237-258.
1137
1138 Olsson, R.K., Hemleben, C., Berggren, W.A. and Huber, B.T., 1999. Atlas of Paleocene Planktonic
1139 foraminifera. Smithsonian Institution Press.
1140
1141 Pearson, P.N., Olsson, R.K., Huber, B.T., Hemleben, C. and Berggren, W.A., 2006. Atlas of Eocene
1142 planktonic foraminifera. Cushman Foundation, Spec. Publ., no. 41.

1143
1144 Peck, R.E. and Forester, R.M., 1979. The genus *Platychara* from the Western hemisphere. Review of
1145 Palaeobotany and Palynology, v. 28, no. 2, p.223-236.
1146
1147 Perch-Nielsen, K., 1979. Calcareous nannofossil zonation at the Cretaceous/Tertiary boundary in
1148 Denmark. In: Birkelund, T. and Bromley, R.G. (eds.), Symposium on the Cretaceous/Tertiary
1149 boundary events; I. The Maastrichtian and Danian of Denmark. Univ. Copenhagen, Denmark, p. 115-
1150 135.
1151
1152 Perch-Nielsen, K., 1985a. Cenozoic calcareous nannofossils. In: Bolli, H.M., Saunders, J.B. and
1153 Perch-Nielsen, K. (eds.), Plankton stratigraphy. Cambridge Univ. Press, p. 427-454.
1154
1155 Perch-Nielsen, K., 1985b. Mesozoic calcareous nannofossils. In: Bolli, H.M., Saunders, J.B. and
1156 Perch-Nielsen, K. (eds.), Plankton stratigraphy. Cambridge Earth Sci. Ser., p. 326-426.
1157
1158 Petrizzo, M.R., Falzoni, F. and Silva, I.P., 2011. Identification of the base of the lower-to-middle
1159 Campanian *Globotruncana ventricosa* Zone: comments on reliability and global correlations.
1160 *Cretaceous Research*, 32(3), pp.387-405.
1161
1162 Pindell, J.L., 1994. Evolution of the Gulf of Mexico and the Caribbean. In: Donovan, S.K. and
1163 Jackson, T.A. (eds.), Caribbean geology: an introduction. University of West Indies Publishers'
1164 Association. Kingston, Jamaica, p. 13-39.
1165
1166 Pindell, J.L., Barrett, S.F., 1990. Geological evolution of the Caribbean region: a plate tectonic
1167 perspective. In: Dengo, G., Case, J.E. (eds.). The Caribbean. Decade of North American Geology,
1168 Boulder, Colorado, Geological Society of America, Volume H, 404-432
1169
1170 Pindell, J., Kennan, L., 2001. Kinematic evolution of the Gulf of Mexico and Caribbean. In: Fillon,
1171 R.H., Weimer, P., Lowrie, A., Pettingill, H., Phair, R. L., Roberts, H.H., van Hoorn, B. (eds.).
1172 Petroleum Systems of Deep-Water Basins: Global and Gulf of Mexico Experience. Gulf Coast Section
1173 Society of Economic Paleontologists and Mineralogists. 21st Annual Bob Perkins Research
1174 Conference, Petroleum Systems of Deep-Water Basins, 193-220.
1175
1176 Pindell, J.L. and Kennan, L., 2009. Tectonic evolution of the Gulf of Mexico, Caribbean and northern
1177 South America in the mantle reference frame: an update. In: James, K.H., Lorente, M.A. and Pindell,

1178 J.L. (eds.), The origin and evolution of the Caribbean Plate. Geol. Soc. Lon. Spec. Publ., v. 328, p. 1-
1179 55.
1180
1181 Pindell, J.L., Kennan, L., Maresch, W.V., Stanek, K-P., Draper, G. And Higgs, R., 2005. Plate-
1182 kinematics and crustal dynamics of circum-Caribbean arccontinent interactions: Tectonic controls on
1183 basin development in Proto-Caribbean margins. Geol. Soc. Am. Spec. Pa. 394, p. 7-52.
1184
1185 Poumot, C., 1989. Palynological evidence for eustatic events in the tropical Neogene. *Bulletin des*
1186 *Centres de Recherches exploration-production Elf-Aquitaine*, 13(2): 437–453.
1187
1188 Premoli-Silva, I. and Verga, D., 2004. Practical manual of Cretaceous planktonic foraminifera.
1189 Tipografia Pontefelcino, Perugia, p. 1-283.
1190
1191 Ramsook, R. and Robinson, E., 2009. A new record of the Paleocene larger foraminifer *Ranikothalia*
1192 *catenula* in the Wagwater Formation of eastern Jamaica. *Caribbean Journal of Earth Science*, v. 40, p.
1193 21-23.
1194
1195 Robaszynski, F. 1998. Planktonic foraminifera-Upper Cretaceous, Chart of Cretaceous
1196 Biochronostratigraphy. In P.-C. de Graciansky, J. Hardenbol and P.R. Vail (Eds.), *Mesozoic and*
1197 *Cenozoic Sequence Stratigraphy of European Basins*. Society for Sedimentary Geology (SEPM),
1198 Special Publication, v. 60, p. 782.
1199
1200 Robinson, E., 2004. Zoning the White Limestone Group of Jamaica using larger foraminiferal genera:
1201 a review and proposal. *Cainozoic Research*, v. 3, no. 1-2, p. 39-75.
1202
1203 Robinson, E. and Mitchell, S.F., 1999. Upper Cretaceous to Oligocene stratigraphy in Jamaica. In:
1204 Mitchell, S. F. (ed.) *Middle Eocene to Oligocene stratigraphy and palaeogeography in Jamaica: A*
1205 *window on the Nicaragua Rise*, Contributions to Geology, UWI, Mona, no. 3, p. 1-47.
1206
1207 Robinson, E. and Wright, R.M., 1993. Jamaican Paleogene larger foraminifera. In: Wright, R. M. and
1208 Robinson, E. (eds.) *Biostratigraphy of Jamaica*. Geol. Soc. Am., v. 182, p. 283-345.
1209
1210 Schlager W (1981) The paradox of drowned reefs and carbonate platforms. *Geol Soc Am Bull*
1211 92(4):197–211
1212

1213 Sigurdsson, H., Leckie, R. M. and Acton, G. D., 1997. Proceedings of the Ocean Drilling Program,
1214 Initial Reports, v. 165.
1215

1216 Sissingh, W., 1977. Biostratigraphy of Cretaceous calcareous nannoplankton. Geol. Mijnbouw, v. 56,
1217 p. 37-65.
1218

1219 Sliter, W.V., 1989. Biostratigraphic zonation for Cretaceous planktonic foraminifers examined in thin
1220 section. J. Foramin. Res., v. 19, no. 1, p. 1-19.
1221

1222 Snedden, J.W., Liu, C., 2010. A compilation of Phanerozoic sea-level change, coastal onlaps and
1223 recommended sequence designations. AAPG Search Discov. Article 40594.
1224

1225 Steineck, P.L., 1974. Foraminiferal palaeoecology of the Montpelier and Lower Coastal Groups
1226 (Eocene-Miocene), Jamaica, West Indies. Palaeogeography, Palaeoclimatology, Palaeoecology, v. 16,
1227 p. 217-242.
1228

1229 Steineck, P. L., 1981, Upper Eocene to middle Miocene ostracode faunas and paleo-oceanography of
1230 the North Coastal Belt, Jamaica: Marine Micropaleontology, v. 6, p. 339-366.
1231

1232 Trechmann, C. T., 1923. The Yellow Limestone of Jamaica and its Mollusca. Geological Magazine, v.
1233 60, p. 337-367.
1234

1235 Wade, B.S., Pearson, P.N., Berggren, W.A. and Pälike, H., 2011. Review and revision of Cenozoic
1236 tropical planktonic foraminiferal biostratigraphy and calibration to the geomagnetic polarity and
1237 astronomical time scale. Earth Science Reviews, v. 55, p. 111-142.
1238

1239 Wadge, G., Jackson, T.A., Isaacs, M.C., Smith, T.E., 1982. The ophiolitic Bath-Dunrobin Formation,
1240 Jamaica: significance for the Cretaceous plate margin evolution in the north-western Caribbean.
1241 Journal of the Geological Society of London, 139, 321-333.
1242

1243 Wescott, W.A. and Ethridge, F.G., 1983. Eocene fan delta-submarine fan deposition in the Wagwater
1244 Trough, east-central Jamaica. Sedimentology, v. 30, no. 2, p.235-247.
1245

1246 Wissler L, Funk H, Weissert H (2003) Response of Early Cretaceous carbonate platforms to changes
1247 in atmospheric carbon dioxide levels. Palaeogeogr Palaeoclimatol Palaeoecol 200(1):187–205
1248

1249 Wright, R. M., 1971. Tertiary biostratigraphy of central Jamaica: tectonic and environmental
1250 implications. In: P. H. Mattson (editor), Trans. 5th Caribbean Geol. Conference (St. Thomas). Geol.
1251 Bull. 5, Queens College Press, Flushing, N.Y., p. 129 (abstract).

